ISSN 2096-7071 (Print)
ISSN 2096-3101 (Online)
CN 10-1629/R1

CHINA CDC WEEKLY

Vol. 6 No. 44 Nov. 1, 2024

中国疾病预防控制中心周报

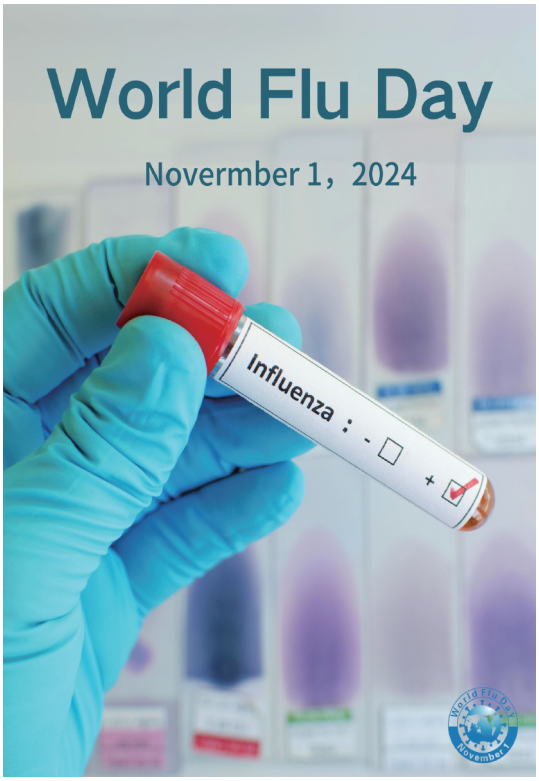

ISSN 2096-7071
9 772096 707248 44>

China CDC Weekly

Cover Image: adapted from Canva, https://www.canva.cn/.

Preplanned Studies

Laboratory-Confirmed Influenza Hospitalizations During Pregnancy or the Early Postpartum Period — Suzhou City, Jiangsu Province, China, 2018–2023

Jinghui Sun[1,2]; Yuanyuan Zhang[2]; Suizan Zhou[3]; Ying Song[3]; Suping Zhang[2]; Jie Zhu[4]; Zhiyuan Zhu[4]; Rui Wang[5]; Hong Chen[6]; Liling Chen[1,2,#]; Haibing Yang[2]; Jun Zhang[7]; Eduardo Azziz-Baumgartner[3]; W. William Schluter[3]

Editorial This report is being published simultaneously in the *Morbidity and Mortality Weekly Report* (https://www.cdc.gov/mmwr/volumes/73/wr/mm7343a1.htm?s_cid=mm7343a1_w).

Summary

What is already known about this topic?

Pregnancy is associated with increased risk for severe illness and complications attributable to influenza infection. Information about the incidence of influenza hospitalization among pregnant and early postpartum women in China is limited.

What is added by this report?

Population-based data from a large city in southern China estimated the annual influenza hospitalization rate to be 2.1 per 1,000 live births. Among hospitalized pregnant and postpartum women with influenza, 86% were admitted to obstetrics rather than respiratory medicine wards; fewer than one third received antiviral treatment. Influenza vaccination coverage among hospitalized pregnant and postpartum women with influenza was <0.1%.

What are the implications for public health practice?

Increasing vaccination coverage among pregnant women can reduce influenza-associated morbidity. Raising awareness about early detection, treatment, and infection control of influenza in obstetrics wards is needed to reduce the adverse impact of influenza on pregnant women.

Worldwide, approximately 200 million women become pregnant each year*. Among women of reproductive age who acquire influenza, those who are pregnant are most likely to experience severe influenza-associated illness (*1*). Despite recommendations by public health agencies, including those in China (*2*), that pregnant women receive an influenza vaccine, in multiple countries where these vaccines are manufactured, licensed, and widely available, influenza vaccination coverage in this population is typically low (*3–4*). Insufficient information about the risk for influenza among pregnant women might contribute to reduced demand for vaccines, and passive sentinel surveillance often underestimates risk because of lack of clarity about catchment areas, insufficient testing, and underreporting (*5*). To estimate the risk for influenza illness in pregnant and postpartum women and to document the proportion of these women who were vaccinated against influenza or received antiviral medications during hospitalization for influenza, analysis of population-based surveillance of influenza hospitalizations among pregnant and early postpartum women was conducted in Suzhou, China.

METHODS

Data Source

The data in this analysis were derived from active population-based surveillance of influenza-associated hospitalizations conducted in Suzhou (population approximately 13 million), a prefecture-level city in China's southern Jiangsu Province, during October 2018–September 2023. The population under surveillance included all pregnant women who sought care in Suzhou and who also were found in the medical record information system, which includes all

* https://population.un.org/wpp.

medical institutions in Suzhou. Cases of acute respiratory or febrile illness (ARFI) among female patients of reproductive age were identified using *International Classification of Diseases, Tenth Revision* codes[†]. Inclusion criteria also included documentation of body temperature ≥99.1 °F (≥37.3 °C) at the time of admission. A wide range of codes and a low temperature threshold were used to capture as many illnesses as possible that were compatible with influenza infection. Pregnancy status was recorded, and nasopharyngeal swabs were collected from all pregnant women and those with a live birth within the preceding 2 weeks (early postpartum) who were hospitalized with ARFI. Laboratory-confirmed influenza-associated ARFI (influenza ARFI) was defined as ARFI with influenza RNA detected by reverse transcription–polymerase chain reaction (RT-PCR) testing of a nasopharyngeal swab [§]. Data on live births were obtained from the Suzhou Bureau of Statistics[¶].

Data Analysis

The annual ARFI hospitalization rate (ARFI hospitalizations per 1,000 live births) was calculated as the annual number of pregnant or postpartum women hospitalized with ARFI divided by the annual number of live births and multiplied by 1,000. Similarly, the annual influenza ARFI hospitalization rate (influenza ARFI hospitalizations per 1,000 live births) was calculated as the annual number of pregnant or postpartum women hospitalized with influenza ARFI divided by the annual number of live births and multiplied by 1,000. To estimate the total ARFI and influenza ARFI rates [with 95% confidence intervals (*CIs*)] among pregnant women in Suzhou, the ratio and 95% *CI* of influenza hospitalizations to total influenza illnesses (i.e., those that were and were not medically attended) from a 2022 cohort study (*3*) in Suzhou (3.2%; 95% *CI*: 1.5%–4.9%) was applied, using bootstrapping. This study was reviewed and approved by the Institutional Review Board of the Chinese Center for Disease Control and Prevention.

RESULTS

Participants and Laboratory Testing

A total of 3,329 pregnant and postpartum women in Suzhou were hospitalized with ARFI[**] during the analysis period, 3,133 (94.1%) of whom had a nasopharyngeal specimen collected (Table 1). Among those who received testing, 495 (15.8%) received a diagnosis of influenza ARFI. Nearly two thirds of patients (325; 65.7%) were infected with an influenza A virus, including 163 (32.9%) with subtype A(H3N2) and 162 (32.7%) with subtype A(H1N1) pdm09. Approximately one third (167, 33.7%) of patients were infected with an influenza B virus, with Victoria lineage virus infection accounting for 157 (94.0% of all influenza B cases and 31.7% of all influenza ARFI cases among pregnant and postpartum women). Among the pregnant and postpartum influenza ARFI patients, 53 (10.7%) cases occurred during the first trimester of pregnancy, 40 (8.1%) during the second trimester, 392 (79.2%) during the third trimester, and 10 (2.0%) during the early postpartum period.

Hospitalization Rates

Among the 495 hospitalized pregnant or postpartum women with influenza ARFI, 479 (96.8%) cases occurred during periods when influenza detection exceeded the epidemic threshold (Figure 1). Influenza ARFI hospitalization rates among pregnant and postpartum women were highest during 2018–2019 (3.4 per 1,000 live births), and lowest during

[†] The *International Classification of Diseases, Tenth Revision* codes to identify ARFI included the following: A41 (sepsis, unspecified), B34 (viral infection, unspecified), B95.3 (*Streptococcus pneumoniae*), B96.0 (*Mycoplasma pneumoniae*), B96.1 (*Klebsiella pneumoniae*), B96.3 (*Haemophilus influenzae*), B97.0 (Adenovirus), B97.2 (Coronavirus), B97.3 (Retrovirus), B97.4 (respiratory syncytial virus), B97.8 (Other viral agents), B99.x01 (Other unspecified infectious diseases), J00–J06 (acute upper respiratory infectious), J09–J18 (influenza and pneumonia), J20–J22 (other acute lower respiratory infections), J35 (chronic diseases of the tonsils and adenoids), J36 (peritonsillar abscess), J39 (other diseases of the upper respiratory tract), J40 (bronchitis, not acute or chronic), J45 (asthma), J46 (status asthmaticus), J80 (acute respiratory distress syndrome), J81 (pulmonary edema), J84 (pulmonary fibrosis, unspecified), J86.9 (pyothorax without fistula), J90 (pleural effusion), J96 (respiratory failure, not classified elsewhere), J98 (other respiratory disorders), O75.1 (shock during or after labor and delivery), O75.2 (pyrexia during labor, not elsewhere classified), O86.4 (pyrexia of unknown origin following delivery), O98.5 (other viral diseases complicating pregnancy, childbirth, and the puerperium), O98.8 (other maternal infectious and parasitic diseases complicating pregnancy, childbirth, and the puerperium), O99.5 (diseases of the respiratory system complicating pregnancy, childbirth, and the puerperium), R04–R07 (hemorrhage from respiratory passages, cough, abnormalities of breathing, pain in throat and chest), R09 (other symptoms and signs involving the circulatory and respiratory system), R50 (fevers of unknown or other origins), R57.9 (shock, unspecified), R65 (systemic inflammatory response syndrome), and R68.8 (other general symptoms and signs).

[§] https://ivdc.chinacdc.cn/cnic/fascc/201802/P020180202290930853917.pdf

[¶] https://tjj.suzhou.gov.cn

[**] Excluding those seen only in emergency departments but not admitted.

TABLE 1. Influenza acute respiratory or febrile illness hospitalization rate and dominant influenza viruses among pregnant or postpartum women* — Suzhou, China, 2018–2023.

Metric	Analysis period					
	Oct 2018–Sep 2019	Oct 2019–Sep 2020	Oct 2020–Sep 2021	Oct 2021–Sep 2022	Oct 2022–Sep 2023	Overall
No. of ARFI hospitalizations	965	570	431	464	899	3,329
No. of live births	68,487	61,916	66,068	53,296	49,724	299,491
Annual ARFI hospitalizations per 1,000 live births (95% *CI*)	14.1 (13.2–15.0)	9.2 (8.5–10.0)	6.5 (5.9–7.2)	8.7 (7.9–9.5)	18.1 (16.9–19.3)	11.1 (10.7–11.5)
No. of sampled and tested ARFI hospitalizations (%)	878 (91.0)	526 (92.3)	417 (96.8)	452 (97.4)	860 (95.7)	3,133 (94.1)
No. of influenza ARFI hospitalizations (%)	233 (26.5)	99 (18.8)	3 (0.7)	77 (17.0)	83 (9.7)	495 (15.8)
Annual influenza ARFI hospitalizations per 1,000 live births (95% *CI*)	3.4 (3.0–3.9)	1.6 (1.3–2.0)	0.05 (0.01–0.13)	1.4 (1.1–1.8)	1.7 (1.3–2.1)	2.1 (1.9–2.3)†
Estimated total annual ARFI cases per 1,000 live births (95% *CI*)§,¶	440.3 (303.7–933.9)	287.8 (196.7–616.9)	203.8 (141.1–440.3)	272.2 (188.7–589.4)	565.0 (391.4–1,204.7)	347.5 (240.3–731.5)
Estimated total annual influenza ARFI cases per 1,000 live births (95% *CI*)§,¶	106.3 (72.6–236.3)	50.0 (33.4–116.4)	1.6 (0.5–7.2)	45.0 (29.4–107.8)	52.2 (34.3–123.3)	65.9 (45.2–142.4)†
Dominant influenza viruses**	A(H1N1)pdm09	B/Victoria	B/Victoria	A(H3N2) and B/Victoria	A(H1N1)pdm09 and A(H3N2)	A(H1N1)pdm09, A(H3N2), and B/Victoria

Abbreviation: ARFI=acute respiratory or febrile illness; influenza ARFI=laboratory-confirmed influenza-associated ARFI; *CI*=confidence interval.

* Less than 2 weeks postpartum.

† Because influenza activity during 2020–2021 did not achieve epidemic levels, these data were excluded from the calculation of the average. The start of each influenza epidemic period was defined as the first day of 3 consecutive influenza reporting weeks in which the percentage of specimens testing positive for any influenza virus infection exceeded 5%. The end of each influenza epidemic period was defined as the day before the first of 3 consecutive influenza reporting weeks during which the percentage of specimens testing positive for influenza was <5%.

§ The total annual ARFI or influenza ARFI rates were estimated through observed hospitalization rates divided by the percentage of hospitalizations among the total number of pregnant or postpartum women with ARFI or influenza ARFI. The percentages of hospitalizations among the total number of pregnant or postpartum women with ARFI or influenza ARFI were assumed the same and equal to the percentage of hospitalizations among the total number of pregnant or postpartum women with influenza (3.2%; 95% *CI*: 1.5%–4.9%). https://pubmed.ncbi.nlm.nih.gov/34323381.

¶ Including cases that were and were not medically attended, outpatients, and inpatients.

** Dominant influenza viruses were defined as those 1) accounting for ≥70% of all isolates during the season or 2) accounting for 40%–70% of all isolates, and the second most common virus accounted for <30%. Subtype/lineage was considered as codominant with the most common virus if it accounted for ≥30% of all isolates.

2020–2021 (0.05 per 1,000 live births). Reported influenza cases in this group of women during 2020–2021, following implementation of coronavirus disease 2019 (COVID-19) nonpharmaceutical interventions (NPIs)[††], were markedly lower than that during other years (P<0.05) and never reached the epidemic threshold. When influenza ARFI hospitalizations among pregnant or postpartum women during 2020–2021 were excluded from the analysis, the average maternal influenza ARFI hospitalization rate for the remaining four influenza seasons was 2.1 per 1,000 live births. The annual average ARFI hospitalization rate was 11.1 per 1,000 live births, including during 2020–2021 (Table 1).

Characteristics of Hospitalized Pregnant or Postpartum Influenza ARFI Patients

Among the 3,329 pregnant or postpartum women who were hospitalized with ARFI, including 495 (14.9%) with influenza ARFI, information on the type of hospital facility was available for 3,133 (94.1%) with ARFI, including all 495 with influenza ARFI (15.8% of the 3,133 with available information). Overall, 2,680 (85.5%) ARFI patients and 423 (85.5%) influenza ARFI patients were admitted to grade III medical institutions, the highest acuity treatment level, which typically treat the most severe cases of illness in China's three-tier health care system[§§] (Table 2). A majority of pregnant and

[††] NPIs to contain COVID-19 in China included three major groups: 1) the restriction of inter-city population movement; 2) the identification and isolation of cases, contact tracing, and quarantine of exposed persons; and 3) the reduction of inner-city travel and contact to increase social distance (e.g., school and workplace closures and cancellation of mass gatherings). https://www.nature.com/articles/s41586-020-2293-x

[§§] https://www.semanticscholar.org/paper/The-Different-Classification-of-Hospitals-Impact-on-Li-Du/937ebf09b1ee8dfbfc18e57ca429d3db8f018325

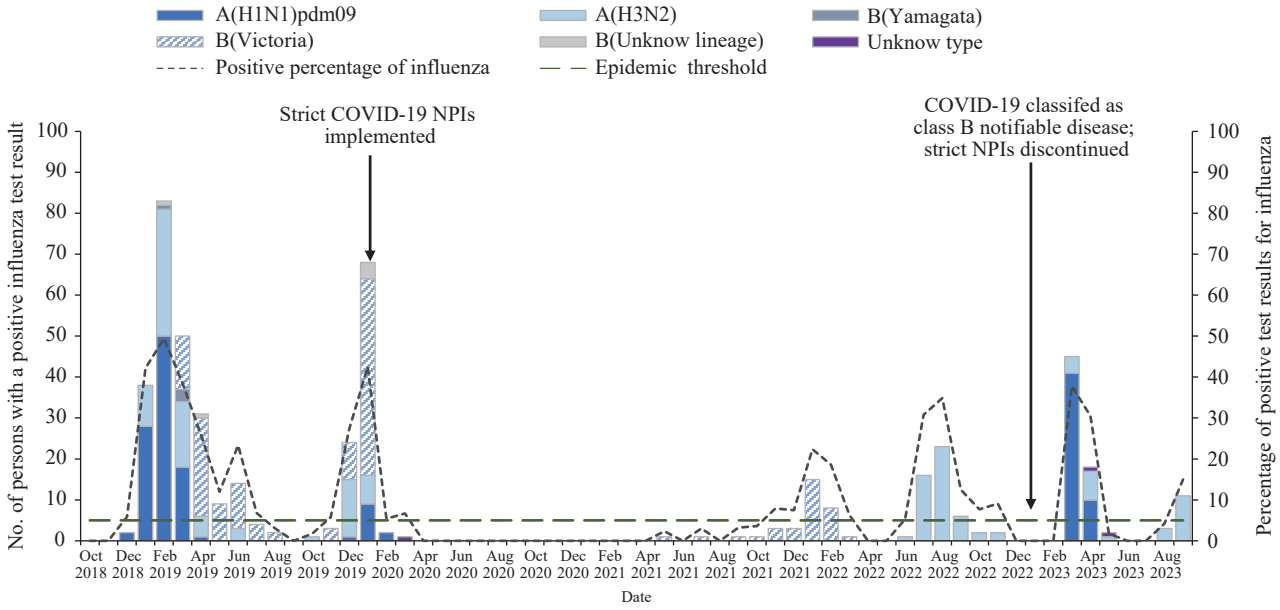

FIGURE 1. Dates of hospitalization of pregnant or postpartum* women, distribution of identified influenza virus subtypes, and implementation of coronavirus disease 2019 (COVID-19) control measures — Suzhou, China, 2018–2023.
* The figure is a combination histogram and line chart showing dates of hospitalization of pregnant or postpartum women, distribution of identified influenza virus subtypes, and implementation of COVID-19 control measures in Suzhou, China during 2018–2023.

postpartum women with ARFI or influenza ARFI were admitted to obstetrics wards (2,588; 82.6% and 423; 85.5%, respectively), rather than to a respiratory medicine ward (299; 9.5% and 37; 7.5%, respectively). Among influenza ARFI patients admitted to obstetrics wards, 371 (87.7%) were in their third trimester.

Among all 3,329 pregnant women with ARFI, only one (0.03%) had received an influenza vaccination, and this vaccinated patient received a negative test result for influenza. Fewer than one third of pregnant or postpartum patients with influenza ARFI (155, 31.3%) received influenza antiviral drug treatment before or during hospitalization. Among 423 women with influenza ARFI hospitalized in an obstetrics ward, 125 (29.6%) received antiviral drug treatment; the highest percentage of women with influenza ARFI admitted to an obstetrics ward who received antiviral treatment were those admitted to a grade III facility (115 of 361 [31.9%]). Among 37 pregnant or postpartum women with influenza ARFI admitted to a respiratory medicine ward, 20 (54.1%) received antiviral treatment. Among 495 influenza ARFI patients, nine (1.8%) were admitted to an intensive care unit; no mechanical ventilation or death cases were reported during hospitalization.

Estimated Total Influenza ARFI Incidence

Estimated total annual influenza ARFI incidence among pregnant and postpartum women, including inpatients or outpatient cases that were and were not medically attended was 65.9 per 1,000 live births. Total annual ARFI incidence was 347.5 cases per 1,000 live births (Table 1).

DISCUSSION

Analysis of active population-based surveillance data for hospitalized pregnant or early postpartum women in Suzhou, China found an annual influenza ARFI hospitalization rate of 2.1 per 1,000 live births. A majority of patients were admitted to obstetrics hospital wards, which are not typically included in respiratory disease surveillance. Influenza ARFI incidence among pregnant and postpartum women, including cases that were and were not medically attended, was estimated to be approximately 70 per 1,000 live births. Only one pregnant woman hospitalized with ARFI had documentation of receipt of influenza vaccination. Fewer than one third of those hospitalized for influenza ARFI were treated with antiviral medications; among patients admitted to obstetrics and gynecology wards, fewer than one third received antiviral medications, compared with approximately one half of those who were admitted to

TABLE 2. Distribution of hospital facilities and wards that cared for pregnant or postpartum* patients with acute respiratory or febrile illness and receipt of antiviral treatment, by hospital grade and ward — Suzhou, China, 2018–2023.

Hospital ward	Institution grade†, no. (%)§							
	Total		Grade I		Grade II		Grade III	
	Total admitted	Received antiviral treatment	Total admitted	Received antiviral treatment	Total admitted	Received antiviral treatment	Total admitted	Received antiviral treatment
ARFI patients								
Total	3,133 (100)¶	331 (10.6)	24 (100)	0 (−)	429 (100)	25 (5.8)	2,680 (100)	306 (11.4)
Obstetrics	2,588 (82.6)	258 (10.0)	13 (54.2)	0 (−)	348 (81.1)	20 (5.7)	2,227 (83.1)	238 (10.7)
Respiratory medicine	299 (9.5)	57 (19.1)	1 (4.2)	0 (−)	23 (5.4)	4 (17.4)	275 (10.3)	53 (19.3)
Gynecology	173 (5.5)	7 (4.0)	10 (41.7)	0 (−)	54 (12.6)	1 (1.9)	109 (4.1)	6 (5.5)
Others	73 (2.3)	9 (12.3)	0 (−)	0 (−)	4 (0.9)	0 (−)	69 (2.6)	9 (13.0)
Influenza ARFI patients								
Total	495 (100)**	155 (31.3)	1 (100)	0 (−)	71 (100)	14 (19.7)	423 (100)	141 (33.3)
Obstetrics	423 (85.5)	125 (29.6)	0 (−)	0 (−)	62 (87.3)	10 (16.1)	361 (85.3)	115 (31.9)
Respiratory medicine	37 (7.5)	20 (54.1)	0 (−)	0 (−)	4 (5.6)	3 (75.0)	33 (7.8)	17 (51.5)
Gynecology	26 (5.3)	6 (23.1)	1 (100)	0 (−)	5 (7.0)	1 (20.0)	20 (4.7)	5 (25.0)
Others	9 (1.8)	4 (44.4)	0 (−)	0 (−)	0 (−)	0 (−)	9 (2.1)	4 (44.4)

Abbreviation: ARFI=acute respiratory or febrile illness; influenza ARFI=laboratory-confirmed influenza-associated ARFI.
* Less than 2 weeks postpartum.
† Hospitals in China are classified into three grades. The lowest is the grade I hospital, which includes primary hospitals and health centers that directly provide prevention, medical care, and rehabilitation services to communities with a certain population. A grade II hospital is a regional hospital that provides comprehensive medical and health services to multiple communities and undertakes certain teaching and research tasks. The highest rank is the grade III hospital, which is a large-scale general hospital with 500 or more beds that integrates medical service, education, and research functions.
§ Percentages in Total admitted columns are column percentages; percentages in Received antiviral treatment columns are percentages of the total number of patients hospitalized in each grade and ward type (e.g., among 348 patients hospitalized in grade II obstetrics wards, 20 (5.7%) received antiviral treatment).
¶ Number of patients (i.e., 94% of 3,329) who had a nasopharyngeal swab collected and for whom information on hospitalization ward was available.
** The 495 influenza ARFI patients were a 15.8% subset of the 3,133 ARFI patients.

respiratory medicine wards.

The annual influenza ARFI hospitalization rate provided important information about influenza-associated inpatient care needs of pregnant or early postpartum women in China. The sentinel influenza surveillance systems in China, which mainly target respiratory medicine wards, have no data collected on pregnancy status or no defined catchment population, given that a majority of sentinel hospitals are large referral hospitals. The clinical diagnosis–based nationally notifiable disease reporting system in China does not report pregnancy status and is subject to significant undertesting and underreporting (*6*). Comparison of influenza hospitalization rates across countries is challenging because of differences in health care–seeking behavior and health care systems. However, the annual rate of community influenza ARFI is more easily compared. The total annual rate of community influenza ARFI among pregnant and early postpartum women (65.9 per 1,000 live births), estimated using data from a 2022 cohort study in Suzhou (*3*), was equivalent to approximately 0.7 cases per 100 person-months (6.6 per 100 person-years). This rate is comparable to recent estimates from community-based prospective cohorts from El Salvador and Panama (5.0 per 100 person-years) (*7*), Kenyan cohorts (0.9–1.2 per 100 person-months) (*8*), the China respiratory illness surveillance among pregnant women cohort (0.7–2.1 per 100 person-months) (*3*), and pregnancy and influenza multinational epidemiologic cohorts from India, Peru, and Thailand (0.7–0.9 per 100 person-months) (*9*), with slight differences possibly attributed to seasonal and geographic variations in this population.

A majority of hospitalized pregnant and postpartum women with ARFI or influenza ARFI were admitted to obstetrics wards, highlighting the importance of including maternity and postnatal wards and departments in sentinel surveillance to estimate influenza ARFI incidence. These estimates suggest that relying on traditional respiratory medicine ward surveillance would have missed approximately 85% of influenza hospitalizations among pregnant or postpartum patients. A strength of this evaluation is that it covered all hospitals in Suzhou and provided testing for influenza by RT-PCR for all pregnant or postpartum patients with ARFI. The methods described here could be used in other settings to accurately estimate the morbidity associated with severe influenza among pregnant women. Accurate estimates can help guide vaccination efforts in groups at risk for severe illness, as well as treatment of pregnant and postpartum women with influenza.

Based on influenza vaccine effectiveness data (*10*), approximately 40% of maternal influenza hospitalizations would have been vaccine-preventable; however, pregnant women were rarely vaccinated. Influenza vaccination coverage among the approximately 18 million pregnant women in China each year[¶¶] is 0.04% (95% *CI*: 0.02%–0.08%), in part because awareness about the risk for influenza illness is low coupled with a lack of demand for influenza vaccination (*3*,*5*). This study confirmed that influenza vaccination coverage among hospitalized pregnant or postpartum women in Suzhou is low. Educating obstetricians about the risks associated with influenza in pregnancy and encouraging them to provide a strong influenza vaccination recommendation for women who are or will be pregnant during the influenza season could help prevent severe influenza morbidity.

The study further found that fewer than one third of pregnant or postpartum patients in Suzhou were treated with influenza antiviral medication even after the diagnosis of influenza; these percentages were lowest among pregnant and postpartum women hospitalized in obstetrics and gynecology wards. Cost and limited availability of the medications, as well as concerns about potential side effects of treatment or risk to the fetus might also have contributed to low antiviral drug treatment for influenza in this population, although multiple observational studies of treatment with oral oseltamivir or zanamivir during pregnancy have not shown a risk to the fetus[***]. In addition to addressing safety concerns, cost-benefit evaluation of antiviral drug treatment for persons at increased risk for influenza complications who seek care at, for example, urgent care centers, might also help increase use of antiviral drugs and limit the occurrence of severe illness. The study findings warrant educating health care providers, especially those working in obstetrics wards, about treatment with antivirals for pregnant or postpartum women with influenza.

These estimates could also be incorporated into vaccine and antiviral cost-benefit analyses to help health authorities assess the return on investment, particularly when compared with more familiar traditional Chinese medicines and supportive care, and to assess the costs and benefits of NPIs (e.g., maintaining good respiratory hygiene, avoiding close contact with persons who have signs or symptoms of influenza-like illness, and minimizing gatherings in crowded places). Implementation of such NPIs during the COVID-19 pandemic might have reduced the risk for infection and spread of influenza.

Limitations

The findings in this report are subject to at least two limitations. First, the study was conducted in a single large city, and the findings might not be generalizable to the rest of China. The study site is economically developed, and health-seeking behavior might vary in other parts of the country. However, it is expected that other, less developed areas with insufficient supplies of vaccine, testing kits, or antiviral drugs, would also experience substantial influenza illnesses and would be less likely to use these specific tools for early detection and protection of pregnant women against influenza. Therefore, these findings might underestimate the incidence of influenza ARFI among pregnant and postpartum women in other parts of the country. Second, the study design did not allow for the inclusion of patients with influenza who might have died or had a fetal loss associated with the hospitalization, which might have underestimated the severe impact of failure to vaccinate and treat pregnant women with influenza.

[¶] https://www.unfpa.org/data/sowmy/CN

[***] https://www.cdc.gov/flu/professionals/antivirals/avrec_ob.htm

Implications for Public Health Practice

The population-based active surveillance outlined in this report underscores the substantial risk for influenza illness among pregnant and postpartum women in China and the potential benefit to pregnant women of offering annual influenza vaccination in prenatal care facilities. Influenza in pregnant women is associated with higher morbidity and mortality. In addition, pregnant women with influenza-like illness might not seek care in respiratory clinics or wards. Increasing awareness of when to seek care for suspected influenza illness, the benefits of early detection and treatment, and infection control in facilities, including prenatal care clinics or wards, could help reduce maternal morbidity during influenza epidemics. Receipt of annual influenza vaccination by pregnant women can prevent influenza-associated morbidity and hospitalization (*10*).

All authors have completed and submitted the International Committee of Medical Journal Editors form for disclosure of potential conflicts of interest.

Conflicts of interest: No conflicts of interest.

doi: 10.46234/ccdcw2024.231

[#] Corresponding author: Liling Chen, liling_chen@163.com.

[1] School of Public Health, Nanjing Medical University, Nanjing, Jiangsu Province, China; [2] Suzhou Center for Disease Control and Prevention, Suzhou City, Jiangsu Province, China; [3] Influenza Division, National Center for Immunization and Respiratory Diseases, CDC, US; [4] Suzhou Health and Family Planning Statistics Information Center, Suzhou City, Jiangsu Province, China; [5] School of Public Health, Xuzhou Medical University, Xuzhou City, Jiangsu Province, China; [6] Chinese Center for Disease Control and Prevention, Beijing, China; [7] Suzhou No.5 People's Hospital, Suzhou City, Jiangsu Province, China.

Submitted: September 10, 2024; Accepted: October 16, 2024

REFERENCES

1. Jamieson DJ, Honein MA, Rasmussen SA, Williams JL, Swerdlow DL, Biggerstaff MS, et al. H1N1 2009 influenza virus infection during pregnancy in the USA. Lancet 2009;374(9688):451 – 8. https://doi.org/10.1016/S0140-6736(09)61304-0.
2. National Immunization Advisory Committee (NIAC) Technical Working Group, Influenza Vaccination TWG. Technical guidelines for seasonal influenza vaccination in China (2023-2024). Chin J Epidemiol 2023;44(10):1507 – 30. https://doi.org/10.3760/cma.j.cn112338-20230908-00139.
3. Chen LL, Zhou SZ, Bao L, Millman AJ, Zhang ZW, Wang Y, et al. Incidence rates of influenza illness during pregnancy in Suzhou, China, 2015-2018. Influenza Other Respir Viruses 2022;16(1):14 – 23. https://doi.org/10.1111/irv.12888.
4. Chen LL, Zhou SZ, Zhang ZW, Wang Y, Bao L, Tan YY, et al. Cohort profile: China respiratory illness surveillance among pregnant women (CRISP), 2015–2018. BMJ Open 2018;8(4):e019709. https://doi.org/10.1136/bmjopen-2017-019709.
5. Zhou SZ, Greene CM, Song Y, Zhang R, Rodewald LE, Feng LZ, et al. Review of the status and challenges associated with increasing influenza vaccination coverage among pregnant women in China. Hum Vaccin Immunother 2020;16(3):602 – 11. https://doi.org/10.1080/21645515.2019.1664230.
6. Huo X, Zhu FC. Influenza surveillance in China: a big jump, but further to go. Lancet Public Health 2019;4(9):e436 – 7. https://doi.org/10.1016/S2468-2667(19)30158-6.
7. Azziz-Baumgartner E, Veguilla V, Calvo A, Franco D, Dominguez R, Rauda R, et al. Incidence of influenza and other respiratory viruses among pregnant women: a multi-country, multiyear cohort. Int J Gynecol Obstet 2022;158(2):359 – 67. https://doi.org/10.1002/ijgo.14018.
8. Otieno NA, Nyawanda BO, McMorrow M, Oneko M, Omollo D, Lidechi S, et al. The burden of influenza among Kenyan pregnant and postpartum women and their infants, 2015–2020. Influenza Other Respir Viruses 2022;16(3):452 – 61. https://doi.org/10.1111/irv.12950.
9. Dawood FS, Kittikraisak W, Patel A, Rentz Hunt D, Suntarattiwong P, Wesley MG, et al. Incidence of influenza during pregnancy and association with pregnancy and perinatal outcomes in three middle-income countries: a multisite prospective longitudinal cohort study. Lancet Infect Dis 2021;21(1):97 – 106. https://doi.org/10.1016/S1473-3099(20)30592-2.
10. Thompson MG, Kwong JC, Regan AK, Katz MA, Drews SJ, Azziz-Baumgartner E, et al. Influenza vaccine effectiveness in preventing influenza-associated hospitalizations during pregnancy: a multi-country retrospective test negative design study, 2010–2016. Clin Infect Dis 2019;68(9):1444 – 53. https://doi.org/10.1093/cid/ciy737.

Preplanned Studies

Social Network Analysis of a Norovirus Outbreak at a Primary School — Zhuhai City, Guangdong Province, China, 2023

Xiling Yin[1]; Songjian Xiao[1]; Xuebao Zhang[1]; Feng Ruan[1,#]

Summary

What is already known about this topic?

The investigations and analyses limited to epidemiological characteristics are insufficient to analyze the spread patterns of norovirus outbreaks in schools.

What is added by this report?

Norovirus outbreaks in primary schools are a dynamic process that spreads through social networks. The use of a social network analysis method to measure and identify key nodes for simulating control evolution was proven effective.

What are the implications for public health practice?

Infected students exhibit priority connection characteristics at different developmental stages in the network topology. Identifying and deliberately targeting key nodes could destroy network connectivity and help reduce the spread of the outbreak.

Norovirus is currently considered the leading cause of acute gastroenteritis worldwide (*1*). Clustering among children in schools can easily lead to norovirus outbreaks (*2*). Rapid and effective control of such outbreaks in schools remains a significant public health challenge (*3*). Norovirus spread should be regarded as a diffusion behavior in social networks and as a dynamic, continuously evolving process. Social network analysis, as a highly flexible research method, can recognize the inherent complexity of individuals' connections. By simulating the transmission dynamics of social networks based on a norovirus outbreak in a primary school, 12 key nodes were identified during the spread and recession periods. This approach demonstrated that targeted control strategies, which transcend inherent epidemiological approaches, are effective and provide insights for emergency management.

Using data from a norovirus outbreak reported in a Zhuhai City primary school (*4*), the epidemic lifecycle — from emergence to spread and decline — was analyzed. A 63×63 transmission matrix was constructed for all nodes. Network analysis and characteristic parameter calculation were performed using UCINET (version 6.528, Analytic Technologies, USA). NetLogo (version 3D 6.1.1, Northwestern's Center for Connected Learning and Computer-Based Modeling, USA) was used to model and simulate the effects of interventions during different epidemic periods. Methods for social network analysis and modeling are described in Supplementary Material (available at https://weekly.chinacdc.cn/).

The norovirus outbreak lasted 23 days, with 63 total cases reported across 6 grades and 18 classes. The class attack rate ranged from 1.96% (1/51) to 42.9% (21/49), and the overall attack rate was 4.2% (63/1,500). The outbreak initially affected 21 cases (Cases 1–21) in 3 classes over 2 days. This initial outbreak was primarily concentrated in Grade 3, Class 3, involving 19 cases, including the index case who experienced vomiting in the classroom on October 13, 2020. The incidence curve indicated a point-source exposure pattern. On October 14, classes for Grade 3, Class 3 were suspended. However, the epidemic continued with a spreading period involving 28 cases (Cases 22–49) across 13 classes over 9 days, suggesting a person-to-person transmission model. On-campus housing was suspended until the evening of October 23. On October 24, a recession period began, involving 14 cases (Cases 50–63) in 10 classes. This period lasted 12 days, and the epidemic curve showed a tailing pattern (Figure 1).

A rapid point-source outbreak occurred in Grade 3, Class 3, with 10 (Cases 2, 5, 7, 11–15, 19, and 20) of the 21 reported cases involved in mixed-class hosting at the school on October 13 and 14, 2020. This activity resulted in the direct infection of 19 students in other classes. The outbreak spread further to the classes of these students and through off-campus hosting centers. Case 23, which was hosted at hosting centers B and C at midday and in the evening, may have caused internal transmission at these two centers. None of the reported cases in Grade 3, Class 3, were cared for at hosting centers A and C. These two centers had longer

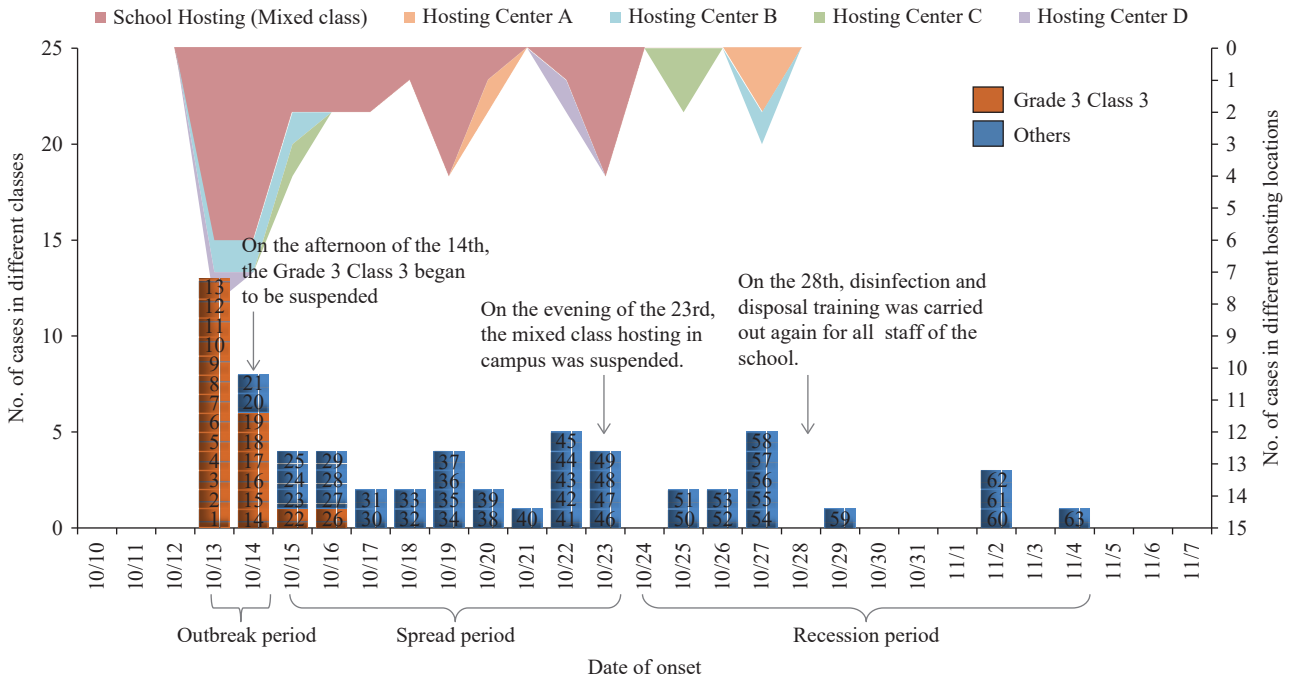

FIGURE 1. The onset date in different classes and hosting locations and periods of development of a norovirus outbreak at a primary school in Zhuhai City, Guangdong Province, China, 2023.

transmission chains. Additionally, Case 9 in Grade 3, Class 3, and Case 43 in Grade 6, Class 2, were both at hosting center D; however, their 8-day onset time interval suggests latent infections within the network as possible sources or bridges of infection. Notably, Case 61 in Grade 6, Class 3, had no clear social relationships within the network (Figure 2).

During the outbreak period, the network was the tightest (density=0.871), with 10 main key nodes (cases 2, 5, 7, 11–15, 19, and 20), which were included in 17 core nodes, as shown by the core-periphery analysis results. The average distance between nodes in the outbreak period was 1.085, meaning any two nodes could communicate through an average of 1.1 intermediate nodes. During the spread period, network tightness decreased (density=0.495), and cases 9, 43, 23, 3, 16, 2/5/7/11–15/19/20 had greater betweenness centralization, meaning they were in a relatively central position in the network. During the recession period, the network was relatively loose (density=0.099). Five core nodes (41, 46–49) were in the core matrix, and cases 48 and 59 were the key nodes as the spread of vomiting according to social network topology. The degree and closeness centralization indicators of the whole network both point to key nodes 2, 5, 7, 11–15, 19, and 20. The average distance was 2.292, and 29 of the 63 cases were in the core matrix (Table 1, Figure 3).

The curve generated with 10 randomly controlled nodes (decay step length=1,083) was similar to the curve generated without controlling any nodes (1,091). Controlling 10 key nodes (2, 5, 7, 11–15, 19, and 20) and eliminating the factors of mixed-class hosting at school significantly reduced the step length of the curve (819). Eliminating the key nodes (48,59) are controlling the spread of vomiting during the recession period further reduced the step length (680) (Figure 4).

DISCUSSION

The network density of the norovirus outbreak gradually decreased from 0.871 to 0.099. This change was likely due to the concentration of cases within a single class during the outbreak period. As the outbreak progressed to the spread period, more classes were involved due to mixed-class activities at school and off-campus hosting. During the recession period, sporadic cases arose, likely due to the untimely isolation of infected individuals and improper handling of vomitus. Previous studies have identified risk factors for norovirus outbreaks in schools, including vomiting on campus and case activity in public areas (*5*). In this outbreak, mixed-class hosting during the spread period and the failure to standardize the handling of vomitus during the recession period were key factors

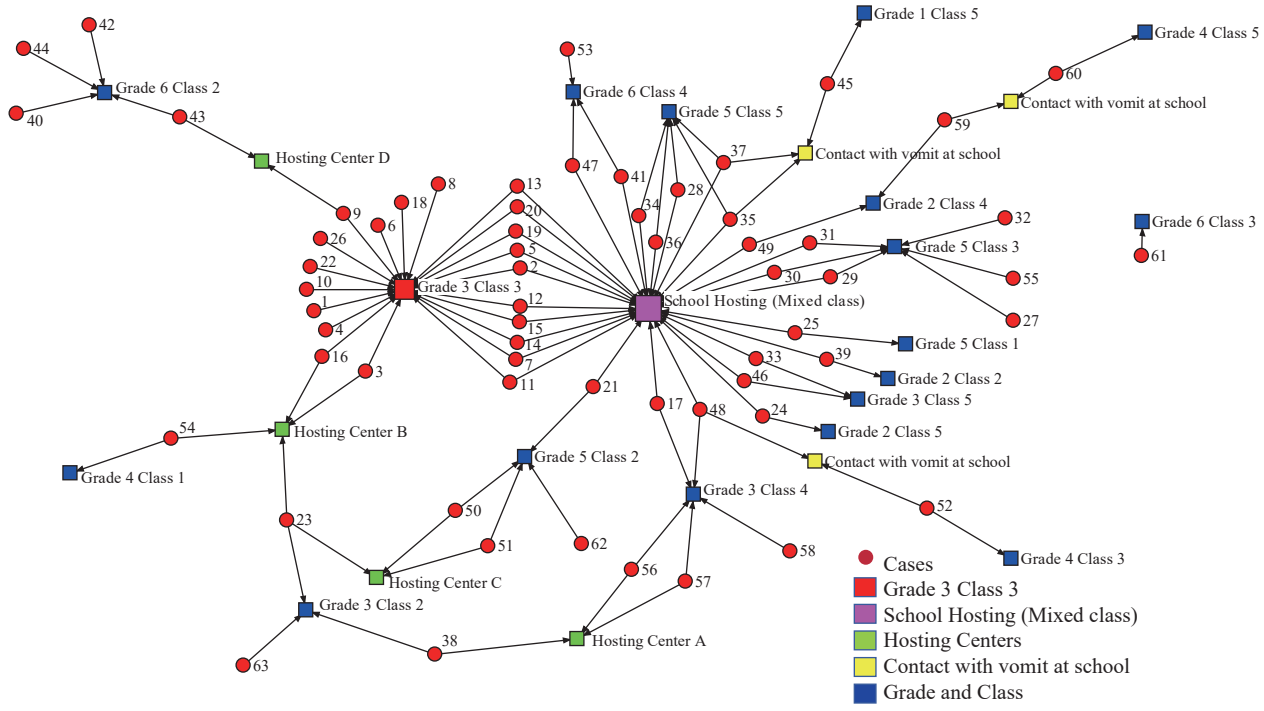

FIGURE 2. The social network topology of 63 cases of a norovirus outbreak at a primary school in Zhuhai City, Guangdong Province, China, 2023.

TABLE 1. The social network characteristic parameters and key nodes of different periods of development of a norovirus outbreak at a primary school in Zhuhai City, Guangdong Province, China, 2023.

Period	Density	Degree centralization		Betweenness centralization	Closeness centralization		Average distance	Core-periphery
		Out	In		Out	In		
Outbreak	0.871	0.083	0.135	0.005	0.502	0.890	1.085	17 core nodes: 2–9, 11–16, 18–20
		Rank 1–10: 2, 5, 7, 11, 12, 13, 14, 15, 19, 20						
Spread	0.495	0.303	0.324	0.139	0.274	0.579	1.793	27 core nodes: 2, 5, 7, 11–15, 19–21, 24, 25, 28–31, 33–37, 39, 41, 46, 47, 49
		Rank 1–10: 2, 5, 7, 11, 12, 13, 14, 15, 19, 20		Rank 1–10: 9, 43, 23, 3, 16, 2/5/7/11–15/19/20	Rank 1–10: 2, 5, 7, 11, 12, 13, 14, 15, 19, 20			
Recession	0.099	0.229	0.324	0.119	0.666	0.664	2.292	5 core nodes: 41, 46–49
		Rank 1–10: 48, 47, 41, 49, 53, 46, 56, 42, 58, 57		Rank 1–7: 48, 53, 49, 42, 41, 47, 59; Other node: 0	Rank 1–10: 52, 53, 41, 47, 48, 49, 46, 60, 56/57/58	Rank 1–10: 42, 43, 44, 48, 49, 41, 47, 46, 56/57/58		
Whole network	0.314	0.304	0.320	0.085	0.125	0.306	2.100	29 core nodes: 2, 5, 7, 11–15, 17, 19–21, 24, 25, 28–31, 33–37, 39, 41, 46–49
		Rank 1–10: 2, 5, 7, 11, 12, 13, 14, 15, 19, 20		Rank 1–10: 9, 43, 23, 48, 3, 16, 17, 49, 21, 29/31/30	Rank 1–10: 2, 5, 7, 11, 12, 13, 14, 15, 19, 20			

contributing to the outbreak and the tailing of the epidemic curve. These factors created critical nodes in the transmission network with priority connection characteristics, increasing the likelihood of disease spreading at each stage. Based on theoretical parameters and operational feasibility, we selected 10 key nodes in the transmission network as primary targets for spread control and 2 key nodes for regression control. Modeling simulations demonstrated that implementing corresponding control measures could effectively reduce the extent and spread of the norovirus.

Social network studies have contributed significantly to understanding the occurrence and development of infectious diseases in recent years (*6*). Studies have shown that immunizing or isolating a small number of nodes can effectively control infectious disease outbreaks (*7*–*8*). This study analyzed the social

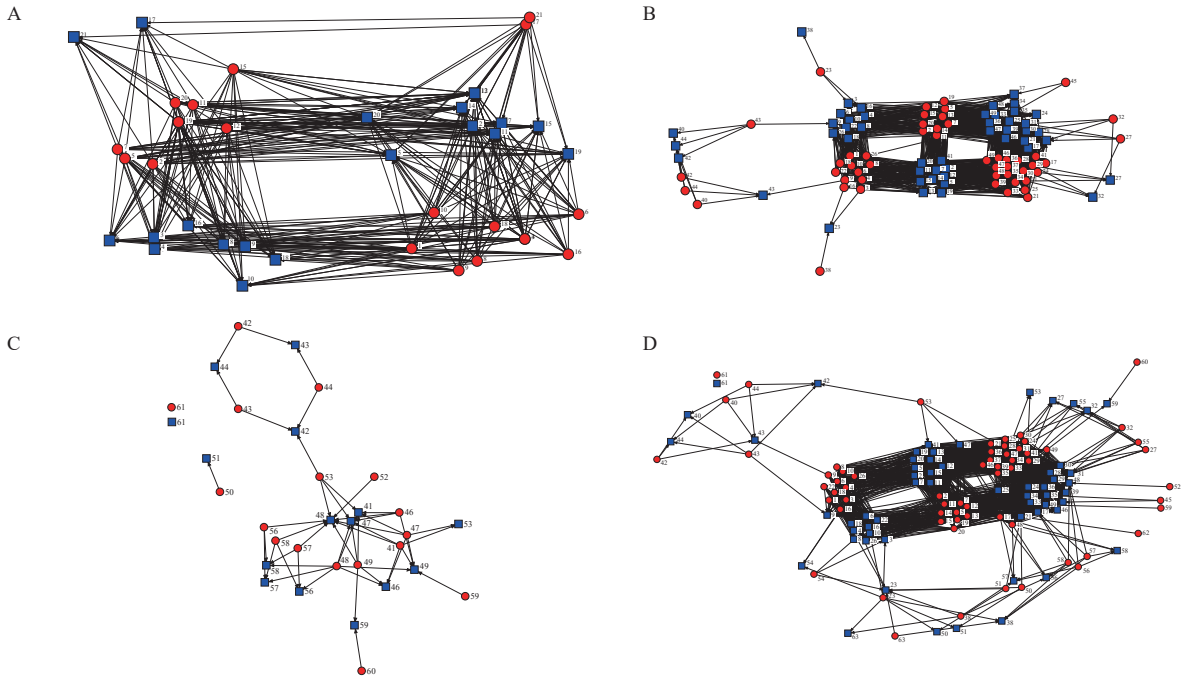

FIGURE 3. The social network matrix of different periods of development of a norovirus outbreak at a primary school in Zhuhai City, Guangdong Province, China, 2023. (A) Outbreak; (B) Spread; (C) Recession; (D) Whole network.

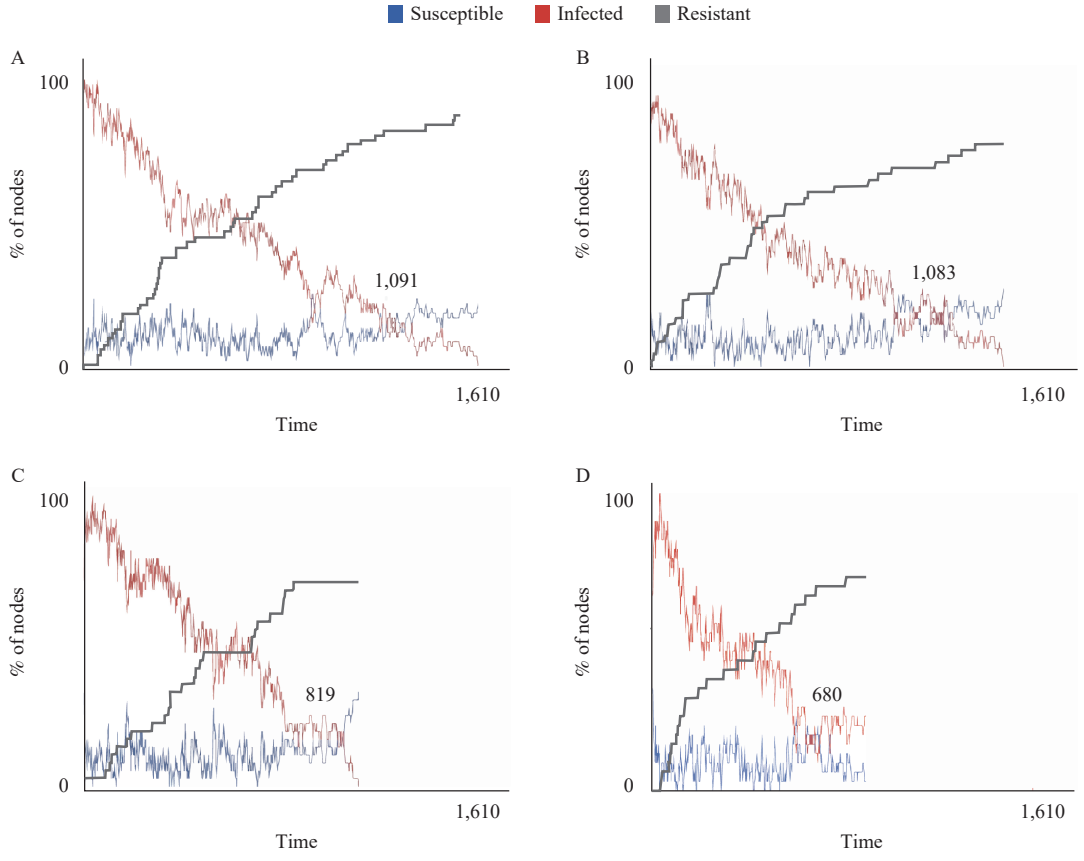

FIGURE 4. The modeling network status of different situations of a norovirus outbreak at a primary school in Zhuhai City, Guangdong Province, China, 2023. (A) Actual situation; (B) Ten random controlled nodes; (C) During the spread period, 10 key nodes (cases 2, 5, 7, 11–15, 19, and 20) were controlled; (D) Control of 10 key nodes and 2 key nodes (cases 48 and 59) in the recession period.

network spread patterns and relationships of 63 cases to verify the effectiveness of this approach in identifying network structures, clarifying core members, and improving decision-making. Using social network analysis, researchers can feasibly identify core nodes and key relationships in infectious disease transmission to accurately and quickly interrupt transmission pathways and prevent large-scale spread or new outbreaks by bridging crowds.

Case 61, who lacked clearly defined social relationships, appeared peripherally in the network. Additionally, despite exhibiting social relationships, some nodes within the network had symptom onset intervals exceeding the incubation period. Notably, studies have reported that latent norovirus infections can account for up to 17.6% of outbreak cases (*9*). Therefore, latent infection within the network may represent a potential source of transmission.

This survey did not include collecting and testing of samples from healthy students or school staff for norovirus nucleic acid, precluding assessment of the proportion of latent infections. Factors such as inadequate vomit disposal practices during the initial stages, non-standard disinfection protocols, and cross-contamination from shared mop use between classes may confound the assessment of network relationships.

CDC physicians might consider incorporating social network analysis when managing norovirus outbreaks in schools. Understanding transmission patterns to identify and control key nodes could help to terminate outbreaks expeditiously.

Conflicts of interest: No conflicts of interest.

Funding: Supported by the Medical Science and Technology Research Fund Project of Guangdong Province (A2021021).

doi: 10.46234/ccdcw2024.232

[#] Corresponding author: Feng Ruan, jkzxrf@zhuhai.gov.cn.

[1] Department of Health Emergency Management, Center for Disease Control and Prevention of Zhuhai City, Zhuhai City, Guangdong Province, China.

Submitted: April 03, 2024; Accepted: October 24, 2024

REFERENCES

1. Tan MD, Tian Y, Zhang DT, Wang QY, Gao ZY. Aerosol transmission of norovirus. Viruses 2024;16(1):151. https://doi.org/10.3390/v16010151.
2. Jin M, Wu SY, Kong XY, Xie HP, Fu JG, He YQ, et al. Norovirus outbreak surveillance, China, 2016-2018. Emerg Infect Dis 2020;26(3):437 – 45. https://doi.org/10.3201/eid2603.191183.
3. Liu J. Whole network approach-a practical guide to UCINET. 3nd ed. Shanghai: Shanghai People's Publishing House 2019. (In Chinese). https://weread.qq.com/web/bookDetail/b37321b0811e3e505g01678.
4. Xiao SJ, Yin XL, Lin XT, Liu DM, Wu YF, Ruan F. Investigation and analysis of an outbreak of norovirus infection in a School. Henan J Prev Med 2022;33(10):768 – 71. https://doi.org/10.13515/j.cnki.hnjpm.1006-8414.2022.10.010.
5. Liu BW, Wang Y, Tan MD, Boran E, Zhang DX, Yan HQ, et al. Risk factors for norovirus outbreaks in schools and kindergartens-Beijing municipality, China, July 2017–June 2022. China CDC Wkly 2024;6(33):841-5. https://weekly.chinacdc.cn/en/article/doi/10.46234/ccdcw2024.181.
6. Liu MX, He SS, Sun YZ, Liu MX, He SS, Sun YZ. The impact of media converge on complex networks on disease transmission. Math Biosci Eng 2019;16(6):6335 – 49. https://doi.org/10.3934/mbe.2019316.
7. Morone F, Makse HA. Influence maximization in complex networks through optimal percolation. Nature 2015;524(7563):65 – 8. https://doi.org/10.1038/nature14604.
8. Guo WF, Zhang SW, Shi QQ, Zhang CM, Zeng T, Chen LN. A novel algorithm for finding optimal driver nodes to target control complex networks and its applications for drug targets identification. BMC Genomics 2018;19(Suppl 1):924. https://doi.org/10.1186/s12864-017-4332-z.
9. Wang J, Ji ZH, Zhang SB, Yang ZR, Sun XQ, Zhang H. Asymptomatic norovirus infection during outbreaks in China: a systematic review and meta-analysis. J Med Virol 2024;96(1):e29393. https://doi.org/10.1002/jmv.29393.

SUPPLEMENTARY MATERIAL

Social network analysis is a research method used to visualize and analyze relationships and connections between entities or individuals within a network. It has emerged as a key technique in modern sociology (*1*).

Relationship Matrix

Social network analysis characterizes networked structures in terms of nodes (individual actors, people, or things within the network) and the ties, edges, or links (relationships or interactions) that connect them. These relationships or interactions can then be coded and converted into data suitable for network analysis (*2*).

The cases reported were used as the nodes and the relationships (links) between cases were identified in our study. It contained the following situations: ① in the same class, ② co-participation in school hosting (mixed class), ③ co-participation in the same off-campus hosting, or ④ contact with vomit (confirmed by the on-site investigation). The first index case reported was used as the initial node. A 63×63 transmission relationship matrix between each node (case) was established.

Visualizing Network

The social network topology was a visualization that represented the nodes and links of a network as a series of connected points. In our study, information was used to visually identify network factors. The cases that serve as bridges between different groups were shown. Nodes were taken in different shapes, colors, or sizes to reflect different characteristics of the cases (Figure 2 in the main text).

Procedure for using the UCINET 6.528 (*3*): Click on the Visualize→NetDraw→File→Open→UCINET dataset→Network

Characteristic Parameters

The characteristic parameters of the network from the initial outbreak through its spread and eventual decline were analyzed in our study (Table 1 and Figure 3 in the main text).

Density

Density is the percentage of possible links that are present in the network. More dense networks are characterized by having more connections between nodes, with 0 representing a network with no connections, and 1 representing a network where all nodes are connected to each other.

Procedure for using the UCINET 6.528: Click on the Network→Cohesion→Density

Centralization

There are three types of centralization (degree, betweenness, and closeness centralization), each corresponding to a different aspect of connectivity and centrality.

Degree Centralization

Degree centralization represents the number of links that a node has. It can be used to identify the most connected cases in the network. In-degree is the number of in-coming links, or the number of predecessor nodes; out-degree is the number of out-going links, or the number of successor nodes. For degree centralization, higher values mean that the node is more central. These cases are considered popular or active and they often have a strong influence within the network due to their higher values of degree centralization.

Procedure for using the UCINET 6.528: Click on the Network→Centrality and Power→Degree

Betweenness Centralization

Betweenness centralization is a centrality measure based on the number of paths of nodes between other nodes. It measures the extent to which a point is located in the "middle" of the other "point pairs" in the network. It can be used to identify these cases as having a unique position where they connect different parts of the network,

facilitating or controlling the flow of information between others.The higher the values of betweenness centralization, the higher the ability of cases as mediators in the network.

Procedure for using the UCINET 6.528: Click on the Network→Centrality and Power→Betweenness

Closeness Centralization

A measure of how quickly a node can reach every other node in the network via the shortest paths. These nodes can disseminate information or exert influence quickly due to their close proximity to all other nodes. The higher the values of closeness centralization, the more important the cases were in the network.

Procedure for using the UCINET 6.528: Click on the Network→Centrality and Power→Closeness

Average Distance

The average distance is the average length of all shortest paths between all pairs of connected vertices in the corresponding network. It can be used to measure the efficiency of the information flow within the network which means that any two nodes can communicate with each other at an average distance between intermediate nodes.

Procedure for using the UCINET 6.528: Click on the Network→Cohesion→Multiple cohesion measures →Average distance

Core-periphery

Core-periphery analysis can identify which nodes are in the tightly connected core region and which nodes are in the loosely distributed periphery in the whole network.

Procedure for using the UCINET 6.528: Click on the Network→Core/Periphery→Categorical

Modeling Network Status

The modeling network parameters were set as follows: average node degree=10, initial outbreak size=21, and virus spread chance=4.2%.

Procedure for using the NetLogo 6.1.1: Click on the File→Model library→Networks→Virus on a network→Setup parameters→Go

REFERENCES

1. Broda MD, Granger K, Chow J, Ross E. Using social network analysis in applied psychological research: a tutorial. Psychol Methods 2023;28(4):791 – 805. https://doi.org/10.1037/met0000451.
2. Tabassum S, Pereira F S F, Fernandes S, Gama J. Social network analysis: an overview. WIREs: Data Min Knowl Discovery 2018;8(5):e1256. https://doi.org/10.1002/widm.1256.
3. Liu J. Lectures on whole network approach-a practical guide to UCINET. 2nd ed. Shanghai: Shanghai People's Publishing House 2014. http://find.nlc.cn/search/showDocDetails?docId=-7227913879254502304&dataSource=ucs01&query=%E6%95%B4%E4%BD%93%E7%BD%91%E5%88%86%E6%9E%90. (In Chinese).

Outbreak Reports

Emergence of a New Sublineage of *Candida auris* Causing Nosocomial Transmissions — Beijing Municipality, China, March–September 2023

Zhenjia Liu[1,&]; Xinfei Chen[2,&]; Rongchen Dai[3,&]; Yu Bai[1]; Feiyi Liu[3]; Yiying Zhao[2]; Xuesong Shang[2]; Chunxia Yang[1]; Xin Fan[1,#]

Summary

What is already known about this topic?

Candida auris (*C. auris*) is an emerging multidrug-resistant fungal pathogen classified as a global public health threat with notable mortality and nosocomial transmission capacity. In China, the first *C. auris* case was reported from Beijing in 2018. However, large cases of nosocomial transmission have rarely been identified in this municipality.

What is added by this report?

During March–September 2023, *C. auris* was isolated from 17 patients admitted to CY Hospital in Beijing. All strains were resistant to fluconazole and amphotericin B. In addition, three isolates were resistant to echinocandins. Whole-genome sequencing (WGS) analysis revealed that all strains found in this hospital belonged to *C. auris* Clade I. These strains were genetically closely related to the *C. auris* strains reported in two other hospitals in Beijing since 2021, forming a new sublineage different from the Clade I strains causing previous outbreaks in the Eastern Provincial-level administrative divisions and Hong Kong Special Administrative Region.

What are the implications for public health practice?

The dissemination of *C. auris* has become an increasing threat to healthcare facilities in China. The WGS analysis indicates the spread of a unique sublineage of *C. auris* Clade I isolates in Beijing. Further, enhanced surveillance and hospital infection control of *C. auris* are warranted to resolve the public health challenge.

Candida auris (*C. auris*) has emerged as a significant global public health threat, leading to its classification as a Critical Priority pathogen by the World Health Organization (WHO) (*1*). Outbreaks of *C. auris* have been reported in several provincial-level administrative divisions (PLADs) in China, including Liaoning, Anhui, and Guangdong (*2*). This study identified 17 nosocomial cluster cases of *C. auris* at a teaching hospital in Beijing Municipality between March and September 2023. Whole-genome sequencing revealed a novel *C. auris* sublineage responsible for this outbreak, highlighting its dissemination within the city.

INVESTIGATION AND RESULTS

This outbreak was identified at CY Hospital, a tertiary teaching hospital in Beijing with 2,500 inpatient beds. The first *C. auris* case was identified on March 2, 2023, from the urine sample of a 78-year-old male patient (Pt01). Pt01 was admitted to the emergency intensive care unit (EICU) due to coronavirus disease 2019 (COVID-19), followed by severe bacterial pneumonia. He underwent a tracheotomy and was discharged on day 6 after the first positive *C. auris* culture. However, Pt01 was readmitted on March 31, 2023, due to an influenza A infection. During his second hospital stay, *C. auris* was cultured 4 times from the patient's urine samples and once from his central venous catheter (Figure 1 and Supplementary Table S1, available at https://weekly.chinacdc.cn/).

Between March and September 2023, *C. auris* isolates were detected in an additional 16 patients (Pt02 to Pt17) at this hospital (Figure 1 and Supplementary Table S1). A total of 38 *C. auris* strains were collected from the 17 patients (Figure 2 and Supplementary Table S2, available at https://weekly.chinacdc.cn/). The hospital's microbiology laboratory and infection prevention team conducted a retrospective study to investigate transmission. A review of patient medical records indicated that of the 17 patients, 82.4% (14/17) were male, and 88.2% (15/17) were older than 65 years. Moreover, 82.4% (14/17) were critically ill. Notably, 76.5% (13/17) of patients had confirmed *C. auris* infections, including

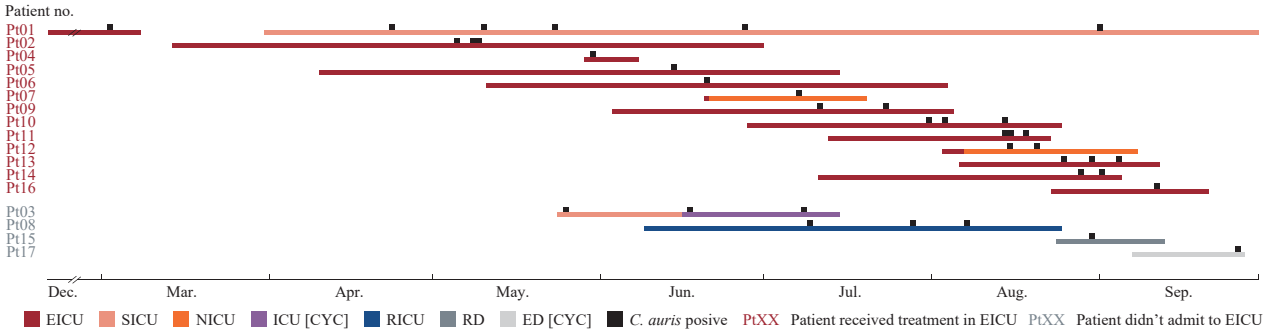

FIGURE 1. Epidemiological timeline of *Candida auris* (*C. auris*)–positive cases identified in the CY Hospital.
Note: This timeline tracked the hospitalization duration and specific clinical wards for each patient and the *C. auris* culture–positive timepoints. Pt01 was admitted to the Emergency Intensive Care Unit of the hospital on December 23, 2022, and the first *C. auris* was isolated from Pt01 on March 2, 2023. Till September 30, 2023, 17 *C. auris*–positive patients were identified in total.

29.4% (5/17) with candidemia and 23.5% (4/17) with *C. auris* colonization. Additionally, 70.6% (12/17) of patients had ≥1 positive urine culture (Supplementary Table S1).

The median duration from patient admission to the first isolation of *C. auris* isolates was 31 days, with an interquartile range of 16–45 days. To better understand the characteristics of *C. auris* nosocomial transmission at the hospital, the investigation team summarized the hospitalization timelines and associated department associations for the 17 positive patients. The investigation revealed that 76.5% (13/17) of patients had a documented history of receiving treatment in the EICU ward, indicating that the EICU may potentially mediate the spread of *C. auris* in the hospital (Figure 1). However, 168 culture-based environmental microbiologic surveillance cultures from the EICU ward, including samples collected before routine ward disinfections, yielded no positive results for *C. auris*. The team also conducted an on-site evaluation focused on infection prevention and control practices in the unit, including the use of personal protective equipment, hand hygiene, processing of reusable medical equipment, and environmental cleaning and disinfection. In general, healthcare personnel adhered to infection control regulations. However, the investigators also observed potential opportunities for contamination of mobile medical devices during patient care and that equipment surface disinfection was sometimes not properly done, which may facilitate the transmission of *C. auris*.

To provide more credible evidence, whole-genome sequencing (WGS) was performed on all 38 isolates using the Illumina Nova 6000 platform in PE150 (150-bp paired-end) sequencing mode (Beijing Novogene Bioinformatics Technology Co., Ltd., China). Additionally, the genomes of 54 Clade I *C. auris* isolates previously reported in China were acquired from the public database (Supplementary Table S3, available at https://weekly.chinacdc.cn/). Single nucleotide polymorphism (SNP) calling and phylogenetic analysis based on WGS data were performed as described previously using the genome of *C. auris* B8441 (GCA_002759435.2_Cand_auris_B8441_V2) as the reference. Detailed laboratory investigation methods are provided in Supplementary Material (available at https://weekly.chinacdc.cn/) (*3*).

WGS analysis revealed that all *C. auris* strains from CY Hospital during this period belonged to Clade I, with 15 to 100 pairwise SNPs between strains (Figure 2). For isolates from the same patient, pairwise SNPs were consistently ≤50. Compared with the genomes of *C. auris* Clade I strains previously reported in China, the strains in this study were genetically similar to those identified from 2 other hospitals in Beijing after 2021 (pairwise SNPs ≤100) but significantly divergent from the first *C. auris* Clade I case reported in Beijing in 2018 (pairwise SNPs >1,000) (Figure 2B). The strains from CY Hospital were also phylogenetically distant from the sublineage of *C. auris* Clade I isolates from the eastern China region (Anhui, Jiangsu, and Shandong provinces) and the outbreak strains recorded in Hong Kong Special Administrative Region (SAR), China, in 2019. Additionally, the strains isolated from 12 of the 13 patients who received treatment in the EICU exhibited more conserved genomic features (pairwise SNPs ≤50) compared with phylogenetic variations against strains from other departments in CY Hospital and other hospitals in Beijing (Figure 2). This molecular evidence further suggests that the rapid dissemination of *C. auris*

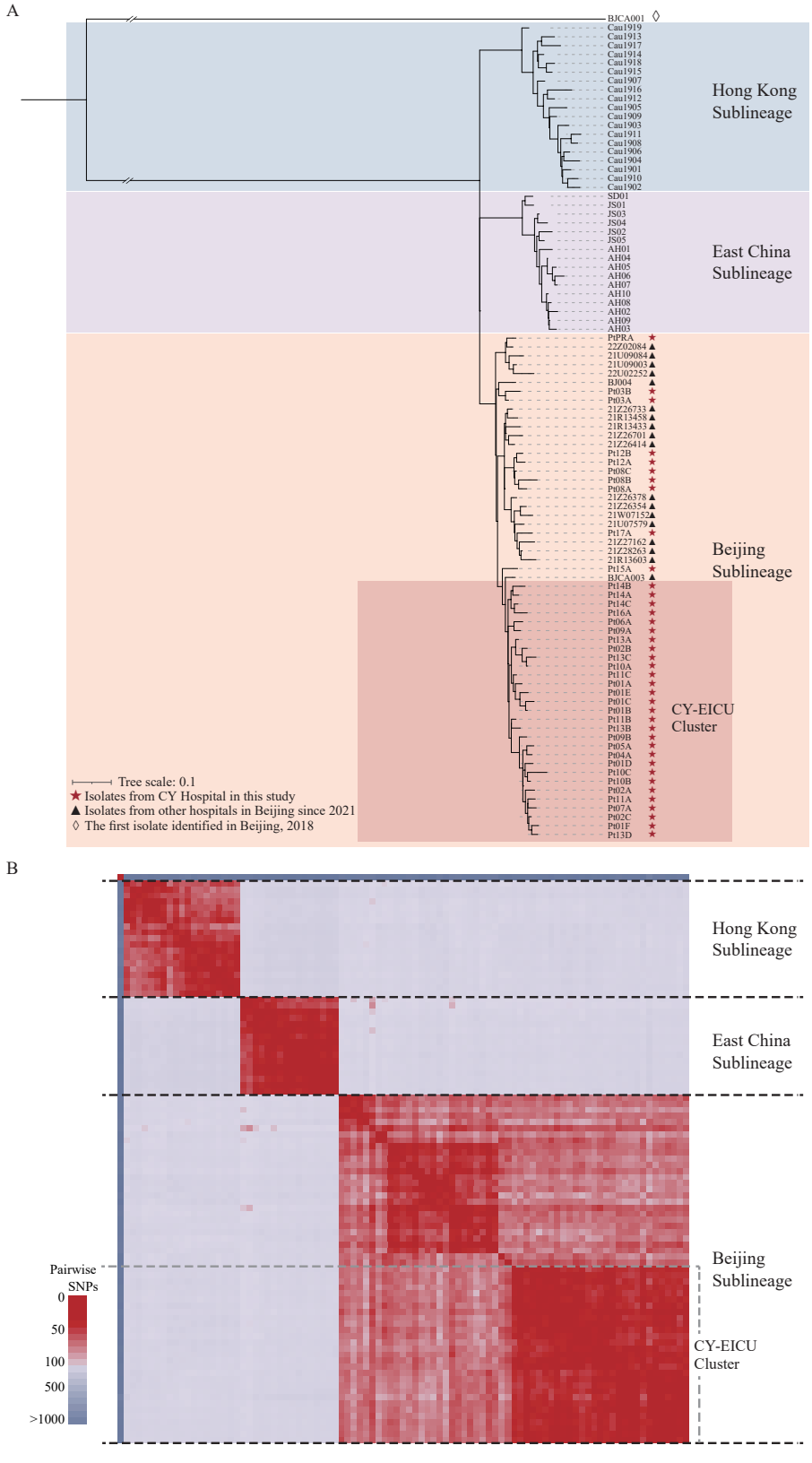

FIGURE 2. Analysis of Clade I *Candida auris* (*C. auris*) isolates in China based on whole-genome sequencing. (A) Phylogenetic tree of *C. auris* Clade I isolates. (B) Heatmap based on genome-wide pairwise SNP analysis, with the order of strains in rows (from top to bottom) and the order in the phylogenetic tree in columns (from left to right).
Note: The first *C. auris* Clade I strain reported in Beijing (BJCA001) was used as root of the phylogenetic tree.

within the EICU may facilitate nosocomial transmission.

Antifungal susceptibility testing suggested that all isolates from CY Hospital were resistant to fluconazole and amphotericin B, according to US CDC tentative breakpoints (Supplementary Table S2). Moreover, WGS analysis revealed that all strains carried the amino acid substitutions Y132F on Erg11 and A583S on Tac1b, both of which are presumed to be associated with azole resistance (*4*–*5*). Of note, the Erg11 Y132F substitution was present in 100% of strains from the Beijing and eastern China sublineages, and 84.2% of strains from the Hong Kong SAR sublineage carried this substitution. In contrast, the Tac1b A583S substitution was found exclusively in the Beijing sublineage and was absent in both the eastern China and Hong Kong sublineage isolates. Additionally, 3 strains from different patients (strains Pt03B, Pt04A, and Pt17A) were echinocandin-resistant, and a key substitution, S639F, on Fks1 (*6*) was observed in 2 of these 3 strains. The overall outcome for these 17 patients was poor, with 35.3% (6/17) of patients dying in the hospital and 29.4% (5/17) showing no improvement before discharge (Supplementary Table S1).

DISCUSSION

C. auris is an emerging multidrug-resistant fungal pathogen that causes life-threatening diseases and nosocomial outbreaks. The crude mortality of invasive infections caused by *C. auris* has exceeded 40%, and the pathogen has rapidly spread to approximately 50 countries worldwide since it was first reported in 2008 (*7*). Notably, the incidence of *C. auris* cases has increased significantly in China since 2023, with several outbreak events reported (*2*). However, most *C. auris* cases reported in Beijing occurred as sporadic events (*2*,*4*–*5*).

In this nosocomial transmission event, 17 *C. auris*-positive patients admitted to the same hospital in Beijing during a 7-month period in 2023 were identified. More than 76% of the cases were confirmed to be *C. auris* infections, and all patients had typical *Candida* infection/colonization risk factors, for example, elderly age or underlying critically ill conditions (*8*–*9*). Patient medical records revealed that >76% of *C. auris*-positive patients received medical management in the EICU ward. As a nosocomial pathogen, *C. auris* has a predilection for colonizing patient skin and can survive on the surface of medical equipment for more than 1 month (*8*). Of note, >70% of patients at CY Hospital had at least one positive urine culture for *C. auris*, with >80% having undergone urinary catheterization. Additionally, on-site investigations in the EICU ward revealed lapses in infection control precautions, such as insufficient disinfection of medical devices and environmental surfaces, which may facilitate the transmission of *C. auris* within the hospital.

WGS is a powerful tool widely used for geographic epidemiology studies and outbreak investigations of microbial pathogens, including fungi. To date, six *C. auris* clades have been categorized globally (Clades I–VI) by WGS (*7*,*10*). In China, *C. auris* Clade I isolates were responsible for several outbreaks that occurred in East China (Anhui, Jiangsu) and Hong Kong SAR, China. In contrast, Clade III isolates caused independent outbreak events in northeastern China (Liaoning Province) and southern China (Guangdong Province) (*2*). As WGS has distinctive discriminatory power, it can provide further insights into the temporal and spatial spread of *C. auris*. In this report, WGS results revealed that the *C. auris* strains isolated in CY Hospital belonged to an emerging sublineage of Clade I, which comprised strains previously found in two other hospitals in Beijing since 2021. This Beijing sublineage had >100 bp SNP differences compared with the Clade I outbreak sublineage in East China and the sublineage spread in Hong Kong SAR. These results indicated that city-wide dissemination of a new *C. auris* sublineage was ongoing in Beijing. Additionally, sporadic cases caused by *C. auris* Clades II and III strains have also been detected in Beijing (*2*), suggesting multiple introductions of diverse lineages of *C. auris* from various sources into the city. As Beijing is a major medical hub receiving patients nationwide for medical services, enhanced surveillance of *C. auris* in the city's healthcare facilities is warranted.

Globally, *C. auris* is highly resistant to fluconazole (>80%) and moderately resistant to amphotericin B (8%–35%) (*1*). Of note, 100% of the strains identified in CY Hospital, as well as strains of the same sublineage in Beijing, were resistant to fluconazole, and all these strains carried substitutions Y132F on Erg11 and A583S on Tac1b (*4*–*5*). In particular, Tac1b A583S represents a unique genomic feature of the Beijing sublineage isolates, distinguishing them from strains of the eastern China and Hong Kong SAR sublineages. Additionally, all but one isolate within the sublineage were amphotericin B resistant. However,

the molecular mechanism responsible for amphotericin B resistance in *C. auris* remains to be investigated. Considering the high possibility of fluconazole and amphotericin B resistance among *C. auris* strains, treatment with echinocandins is currently the preferred method, and echinocandin resistance is rare (*1*). However, in this nosocomial transmission event, we further identified echinocandin-resistant isolates from 3 different patients, and a key substitution, S639F, was found on the hotspot region of Fks1 in 2 of these patients (*6*). Both of these echinocandin-resistant isolates were cultured from urine samples. Their concentration was significantly lower (<1.5%) in urine than in plasma due to the inherent nature of echinocandin-class agents. Consequently, the development of echinocandin resistance in *C. auris* could have been induced by the subtherapeutic low echinocandin concentrations present in urine during treatment (*6*).

A global consensus has emerged recognizing the significant challenges *C. auris* poses to healthcare facilities and public health. This consensus highlights the potential need for more aggressive strategies, including comprehensive surveillance, active case findings, and enhanced infection control measures (*1*). Currently, infection control strategies for *C. auris* generally adhere to standard prevention protocols for other multidrug-resistant organisms. These protocols include routine hand hygiene, environmental disinfection, and contact precautions (*9*). However, the efficacy of these strategies requires further evaluation.

This study has several limitations. First, all environmental samples from the EICU ward were negative for *C. auris*, which limited investigation of potential transmission pathways. These negative results may be due to the limited sensitivity of traditional culture-based methods; molecular tools will be incorporated in future screening efforts. Additionally, healthcare personnel and personal protective equipment have not yet been screened for *C. auris*. Overall, infection control investigations in this case require further enhancement.

In conclusion, as stated in this report, an emerging sublineage of multidrug-resistant Clade I *C. auris* disseminated in Beijing, which was responsible for nosocomial transmission in 17 patients. WGS assays can provide insights into the dynamics of *C. auris* transmission in addition to resistance mechanisms.

Conflicts of interest: No conflicts of interest.

Acknowledgements: The WGS results of *C. auris* isolates in this study are deposited at the NCBI Sequence Read Archive under BioProject ID: PRJNA906339.

Funding: Supported by the National Key Research and Development Program of China (2022YFC2303002), the Reform and Development Program of Beijing Institute of Respiratory Medicine (Ggyfz202418), and the National High-Level Hospital Clinical Research Funding (2022-PUMCH-A-058).

doi: 10.46234/ccdcw2024.233

Corresponding author: Xin Fan, fanxin12356@163.com.

[1] Department of Infectious Diseases and Clinical Microbiology, Beijing Institute of Respiratory Medicine and Beijing Chao-Yang Hospital, Capital Medical University, Beijing, China; [2] Department of Laboratory Medicine, State Key Laboratory of Complex Severe and Rare Diseases, Peking Union Medical College Hospital, Chinese Academy of Medical Sciences, Beijing, China; [3] Graduate School, Peking Union Medical College, Beijing, China.
[&] Joint first authors.

Submitted: September 05, 2024; Accepted: October 28, 2024

REFERENCES

1. World Health Organization. WHO fungal priority pathogens list to guide research, development and public health action. Geneva: WHO; 2022 Oct. https://www.who.int/publications/i/item/9789240060241.
2. Bing J, Du H, Guo PH, Hu TR, Xiao M, Lu S, et al. *Candida auris*-associated hospitalizations and outbreaks, China, 2018-2023. Emerg Microbes Infect 2024;13(1):2302843. https://doi.org/10.1080/22221751.2024.2302843.
3. Fan X, Dai RC, Zhang S, Geng YY, Kang M, Guo DW, et al. Tandem gene duplications contributed to high-level azole resistance in a rapidly expanding *Candida tropicalis* population. Nat Commun 2023;14(1):8369. https://doi.org/10.1038/s41467-023-43380-2.
4. Hong H, Ximing Y, Jinghan M, Al-Danakh A, Shujuan P, Ying L, et al. *Candida auris* infection; diagnosis, and resistance mechanism using high-throughput sequencing technology: a case report and literature review. Front Cell Infect Microbiol 2023;13:1211626. https://doi.org/10.3389/fcimb.2023.1211626.
5. Chen XF, Zhang H, Liu LL, Guo LN, Liu WJ, Liu YL, et al. Genome-wide analysis of in vivo-evolved *Candida auris* reveals multidrug-resistance mechanisms. Mycopathologia 2024;189(3):35. https://doi.org/10.1007/s11046-024-00832-7.
6. Spruijtenburg B, Ahmad S, Asadzadeh M, Alfouzan W, Al-Obaid I, Mokaddas E, et al. Whole genome sequencing analysis demonstrates therapy-induced echinocandin resistance in *Candida auris* isolates. Mycoses 2023;66(12):1079 – 86. https://doi.org/10.1111/myc.13655.
7. Gifford H, Rhodes J, Farrer RA. The diverse genomes of *Candida auris*. Lancet Microbe 2024;5(9):100903. https://doi.org/10.1016/S2666-5247(24)00135-6.
8. Mishra SK, Yasir M, Willcox M. *Candida auris*: an emerging antimicrobial-resistant organism with the highest level of concern. Lancet Microbe 2023;4(7):e482 – 3. https://doi.org/10.1016/S2666-5247(23)00114-3.
9. Wasylyshyn A, Stoneman EK. Management of *Candida auris*. JAMA 2024;331(7):611 – 2. https://doi.org/10.1001/jama.2023.24921.
10. Suphavilai C, Ko KKK, Lim KM, Tan MG, Boonsimma P, Chu JJK, et al. Detection and characterisation of a sixth *Candida auris* clade in Singapore: a genomic and phenotypic study. Lancet Microbe 2024;5(9):100878. https://doi.org/10.1016/S2666-5247(24)00101-0.

SUPPLEMENTARY MATERIAL

METHODS

Antifungal Susceptibility Testing

Minimum inhibitory concentrations (MICs) of nine antifungal agents were measured using Sensititre YeastOne^{TM} YO10 methodology (Thermo Scientific, Cleveland, OH, United States) for all *Candida auris* (*C. auris)* isolates collected in this study. The nine antifungal agents tested included four azoles (fluconazole, voriconazole, itraconazole and posaconazole), three echinocandins (caspofungin, micafungin and anidulafungin), 5-flucytosine and amphotericin B. Current available US CDC tentative breakpoints were applied (https://www.cdc.gov/fungal/candida-auris/c-auris-antifungal.html) for interpretation of susceptibility results. The quality-control strains were *Candida parapsilosis* ATCC 22019 and *Candida krusei* ATCC 6258.

Whole Genome Sequencing and Phylogenetic Analysis

All the isolates collected in this study were subjected to whole genome sequencing (WGS) using Illumina Nova 6000 platform in PE150 (150 bp paired-end) sequencing mode at Beijing Novogene Bioinformatics Technology Co., Ltd. Trimmomatic (version 0.36) was used to remove the adapters and low-quality reads from raw sequencing data (*1*). For each isolate, the reads were mapped to the *C. auris* Clade I strain B8441 (GCA_002759435.2_Cand_auris_B8441_V2) with the Burrows–Wheeler Aligner (BWA version 0.7.7) (*2*). SAMtools (version 1.6) coupled with Genome Analysis Toolkit (GATK version 4.3.0.0) were used for single nucleotide polymorphism (SNP) and indel calling (*3*–*4*). IQ-TREE (version 1.6.12) was used to generate a maximum likelihood (ML) tree of all *C. auris* isolates studied using the 2,373 confident SNPs and 1,000 ultrafast bootstrap replicates (*5*). The script "vcf2phylip.py" (https://github.com/edgardomortiz/vcf2phylip) was used to generate a FASTA for calculating inter-strain pairwise SNPs.

SUPPLEMENTARY TABLE S1. Information on 17 *C. auris*–positive patients from the CY Hospital.

Patient no.	Gender	Age (years)	Critical condition	Experienced treatment in EICU	Infection or colonization	Outcome	Date admitted to the hospital	Hospitalization days to first isolation of *C. auris*	No. of *C. auris* isolates cultured from						
									Total	Urine	Blood	CVC	Drainage	Pus	BALF
Pt01	Male	78	Yes	Yes	Infection	Not improved	2022/12/23	70	6	5		1			
Pt02	Female	86	Yes	Yes	Infection	Dead	2023/3/14	53	3	1		1	1		
Pt03	Male	71	Yes	No	Infection	Improved	2023/5/24	2	2	2					
Pt04	Female	79	Yes	Yes	Colonization	Not improved	2023/5/29	2	1	1					
Pt05	Male	26	Yes	Yes	Infection	Not improved	2023/4/10	66	1					1	
Pt06	Female	86	Yes	Yes	Infection	Improved	2023/5/11	41	1			1			
Pt07	Male	67	Yes	Yes	Infection	Improved	2023/6/20	18	1					1	
Pt08	Male	67	Yes	No	Colonization	Dead	2023/6/9	31	3	3					
Pt09	Male	78	Yes	Yes	Infection	Improved	2023/6/3	39	2	2					
Pt10	Female	82	Yes	Yes	Infection	Improved	2023/6/28	34	3	3					
Pt11	Male	81	Yes	Yes	Infection	Dead	2023/7/13	33	3	1	1				1
Pt12	Female	74	Yes	Yes	Infection	Not improved	2023/8/3	13	2		2				
Pt13	Male	52	Yes	Yes	Infection	Dead	2023/8/6	20	4	1	1	1			
Pt14	Female	83	Yes	Yes	Infection	Dead	2023/7/11	49	3	1	2				
Pt15	Female	84	No	No	Colonization	Improved	2023/8/24	7	1	1					
Pt16	Female	75	Yes	Yes	Infection	Not improved	2023/8/23	20	1		1				
Pt17	Male	74	No	No	Colonization	Not improved	2023/9/7	21	1	1					

Abbreviation: *C. auris* =*Candida auris*; BALF=bronchoalveolar lavage fluid; CVC=central venous catheter.

SUPPLEMENTARY TABLE S2. Information on *C. auris* isolates identified from the CY Hospital.

Strain no.	Patient no.	Department of isolation	Date of sampling	Specimen type	Antifungal susceptibility (minimum inhibitory concentration, mg/L)*									Genome accession no.	Key substitutions	
					Fluconazole	Voriconazole	Itraconazole	Posaconazole	Amphotericin B	Caspofungin	Micafungin	Anidulafungin	5-Flucytosine		Erg11	Fks
Pt01A	Pt01	EICU	2023/3/2	Urine	***128***	0.5	0.12	0.03	***4***	0.12	0.12	0.12	0.12	SRR29824987	Y132F	
Pt01B	Pt01	SICU1	2023/4/23	Urine	***256***	0.5	0.12	0.03	***4***	0.5	0.12	0.25	0.12	SRR29824986	Y132F	
Pt01C	Pt01	SICU1	2023/5/10	Urine	***256***	0.5	0.25	0.06	***2***	0.25	0.12	0.25	<0.06	SRR29824972	Y132F	
Pt01D	Pt01	SICU1	2023/5/23	Urine	***256***	0.5	0.25	0.03	***2***	0.5	0.12	0.25	0.12	SRR29824961	Y132F	
Pt01E	Pt01	SICU1	2023/6/27	Urine	***128***	0.5	0.12	0.03	***2***	0.5	0.12	0.25	0.12	SRR29824951	Y132F	
Pt01F	Pt01	SICU1	2023/9/2	CVC	***256***	0.5	0.12	0.06	***2***	0.5	0.12	0.25	0.12	SRR29824950	Y132F	
Pt02A	Pt02	EICU	2023/5/5	Drainage	***128***	0.5	0.12	0.03	***4***	0.12	0.12	0.25	0.06	SRR29824949	Y132F	
Pt02B	Pt02	EICU	2023/5/8	Urine	***128***	0.25	0.06	0.03	***2***	0.12	0.12	0.12	0.12	SRR29824983	Y132F	
Pt02C	Pt02	EICU	2023/5/9	CVC	***128***	0.5	0.12	0.03	***4***	0.12	0.12	0.12	0.12	SRR29824982	Y132F	
Pt03A	Pt03	SICU2	2023/5/25	Urine	***256***	0.5	0.12	0.03	***4***	0.12	0.12	0.12	0.12	SRR29824981	Y132F	
Pt03B	Pt03	ICU2 [CYC]	2023/6/17	Urine	***128***	0.25	0.06	0.03	***4***	***8***	***>8***	***>8***	<0.06	SRR29824985	Y132F	S639F
Pt04A	Pt04	EICU	2023/5/30	Urine	***128***	0.5	0.06	0.03	***2***	***4***	***>8***	***4***	0.12	SRR29824984	Y132F	S639F
Pt05A	Pt05	EICU	2023/6/14	Pus	***256***	1	0.12	0.06	***4***	0.12	0.12	0.12	0.12	SRR29824980	Y132F	
Pt06A	Pt06	EICU	2023/6/20	CVC	***128***	0.5	0.12	0.03	***4***	0.12	0.12	0.12	0.12	SRR29824979	Y132F	
Pt07A	Pt07	NICU	2023/7/7	Pus	***256***	1	0.25	0.06	***2***	0.25	0.25	0.25	0.12	SRR29824978	Y132F	
Pt08A	Pt08	RICU	2023/7/9	Urine	***>256***	1	0.25	0.06	***2***	0.12	0.12	0.12	<0.06	SRR29824977	Y132F	
Pt08B	Pt08	RICU	2023/7/28	Urine	***>256***	1	0.25	0.12	***4***	0.12	0.12	0.12	0.12	SRR29824976	Y132F	
Pt08C	Pt08	RICU	2023/8/7	Urine	***>256***	1	0.12	0.06	***2***	0.12	0.12	0.12	<0.06	SRR29824975	Y132F	
Pt09A	Pt09	EICU	2023/7/11	Urine	***128***	0.25	0.12	0.03	***2***	0.06	0.12	0.12	<0.06	SRR29824974	Y132F	
Pt09B	Pt09	EICU	2023/7/23	Urine	***128***	0.25	0.06	0.03	***2***	0.12	0.12	0.12	0.06	SRR29824973	Y132F	
Pt10A	Pt10	EICU	2023/7/31	Urine	***128***	0.5	0.06	0.03	***4***	0.12	0.12	0.12	0.12	SRR29824971	Y132F	
Pt10B	Pt10	EICU	2023/8/3	Urine	***256***	1	0.25	0.06	***4***	0.25	0.12	0.25	0.12	SRR29824970	Y132F	
Pt10C	Pt10	EICU	2023/8/14	Urine	***256***	2	0.25	0.06	***2***	0.25	0.12	0.25	0.12	SRR29824969	Y132F	
Pt11A	Pt11	EICU	2023/8/14	Urine	***128***	0.25	0.06	0.03	***4***	0.06	0.12	0.12	0.06	SRR29824968	Y132F	
Pt11B	Pt11	EICU	2023/8/15	BALF	***256***	1	0.12	0.12	***4***	0.12	0.12	0.12	0.12	SRR29824967	Y132F	
Pt11C	Pt11	EICU	2023/8/18	Blood	***128***	0.5	0.12	0.03	***4***	0.12	0.12	0.12	0.12	SRR29824966	Y132F	

Continued

Strain no.	Patient no.	Department of isolation	Date of sampling	Specimen type	Antifungal susceptibility (minimum inhibitory concentration, mg/L)*									Genome accession no.	Key substitutions	
					Fluconazole	Voriconazole	Itraconazole	Posaconazole	Amphotericin B	Caspofungin	Micafungin	Anidulafungin	5-Flucytosine		Erg11	Fks
Pt12A	Pt12	NICU	2023/8/15	Blood	***>256***	0.5	0.12	0.03	***4***	0.25	0.25	0.12	<0.06	SRR29824965	Y132F	
Pt12B	Pt12	NICU	2023/8/20	Blood	***256***	1	0.25	0.06	***2***	0.5	0.12	0.25	0.12	SRR29824964	Y132F	
Pt13A	Pt13	EICU	2023/8/25	Blood	***256***	0.5	0.12	0.03	***4***	0.12	0.12	0.12	0.12	SRR29824963	Y132F	
Pt13B	Pt13	EICU	2023/8/25	CVC	***128***	0.5	0.12	0.03	***4***	0.12	0.12	0.12	0.12	SRR29824962	Y132F	
Pt13C	Pt13	EICU	2023/8/30	Wound	***256***	0.5	0.12	0.03	***4***	0.12	0.12	0.12	0.12	SRR29824960	Y132F	
Pt13D	Pt13	EICU	2023/9/4	Urine	***256***	0.5	0.12	0.03	***4***	0.12	0.12	0.12	0.12	SRR29824959	Y132F	
Pt14A	Pt14	EICU	2023/8/28	Blood	***128***	0.5	0.12	0.03	***4***	0.12	0.12	0.12	0.12	SRR29824958	Y132F	
Pt14B	Pt14	EICU	2023/9/1	Urine	***256***	0.5	0.12	0.03	***4***	0.12	0.12	0.25	0.12	SRR29824957	Y132F	
Pt14C	Pt14	EICU	2023/9/1	Blood	***256***	0.5	0.25	0.06	***2***	0.25	0.12	0.25	0.12	SRR29824956	Y132F	
Pt15A	Pt15	RD2	2023/8/30	Urine	***128***	0.5	0.12	0.06	***4***	0.12	0.12	0.12	0.12	SRR29824955	Y132F	
Pt16A	Pt16	EICU	2023/9/11	Blood	***128***	0.5	0.12	0.03	***4***	0.12	0.12	0.12	0.06	SRR29824954	Y132F	
Pt17A	Pt17	ED [CYC]	2023/9/26	Urine	***>256***	8	0.5	0.25	***4***	***>8***	***2***	***2***	0.12	SRR29824953	Y132F	
PtPRA[†]	PtPR	RD4	2022/3/2	Urine	***>256***	8	0.5	0.25	***8***	0.5	0.25	0.25	0.25	SRR29824952	Y132F	

Abbreviation: *C. auris*=*Candida auris*; ED=emergency department; RD=respiratory department; ICU=intensive care unit; EICU=emergency ICU; NICU=neurology ICU; RICU=respiratory ICU; SICU=surgical ICU; BALF=bronchoalveolar lavage fluid; CVC=central venous catheter.

* Resistant results for fluconazole, amphotericin B and echinocandin agents interpreted per US CDC tentative breakpoints (https://www.cdc.gov/fungal/candida-auris/c-auris-antifungal.html) were marked in italic bold font.

[†] Strain PtPRA was isolated from a patient admitted to the hospital one year before the study period. This patient had been described in another report during treatment at a different hospital (Chen XF et al. 2024), and was not included in the 17 cases reported in this study.

SUPPLEMENTARY TABLE S3. Published *Candida auris* Clade I genomes used in this study.

Genome accession no.	Isolate	Provincial-level administrative divisions	Reference
SRR9316737	BJCA001	Beijing	*6*
ERR3503255	Cau1901	Hong Kong	*7*
ERR3503256	Cau1902	Hong Kong	*7*
ERR3503257	Cau1903	Hong Kong	*7*
ERR3503258	Cau1904	Hong Kong	*7*
ERR3503259	Cau1905	Hong Kong	*7*
ERR3503260	Cau1906	Hong Kong	*7*
ERR3503261	Cau1907	Hong Kong	*7*
ERR3503262	Cau1908	Hong Kong	*7*
ERR3503263	Cau1909	Hong Kong	*7*
ERR3503264	Cau1910	Hong Kong	*7*
ERR3503265	Cau1911	Hong Kong	*7*
ERR3503266	Cau1912	Hong Kong	*7*
ERR3503267	Cau1913	Hong Kong	*7*
ERR3503268	Cau1914	Hong Kong	*7*
ERR3503269	Cau1915	Hong Kong	*7*
ERR3503270	Cau1916	Hong Kong	*7*
ERR3503271	Cau1917	Hong Kong	*7*
ERR3503272	Cau1918	Hong Kong	*7*
ERR3503273	Cau1919	Hong Kong	*7*
SRR20980354	BJCA003	Beijing	*8*
SRR26035613	BJ004	Beijing	*9*
SRR26035602	SD01	Shandong	*9*
SRR26035601	JS01	Nanjing	*9*
SRR26035600	JS02	Nanjing	*9*
SRR26035599	JS03	Nanjing	*9*
SRR26035598	JS04	Nanjing	*9*
SRR26035597	JS05	Nanjing	*9*
SRR26035596	AH08	Anhui	*9*
SRR26035623	AH09	Anhui	*9*
SRR26035622	AH10	Anhui	*9*
SRR26035621	AH04	Anhui	*9*
SRR26035620	AH05	Anhui	*9*
SRR26035619	AH06	Anhui	*9*
SRR26035618	AH07	Anhui	*9*
SRR26035617	AH01	Anhui	*9*
SRR26035616	AH02	Anhui	*9*
SRR26035615	AH03	Anhui	*9*
SRR29536503	21U07579	Beijing	*10*
SRR29536500	21Z28263	Beijing	*10*
SRR29536497	22Z02084	Beijing	*10*
SRR29536494	21Z26378	Beijing	*10*

Continued

Genome accession no.	Isolate	Provincial-level administrative divisions	Reference
SRR29536491	21Z26701	Beijing	*10*
SRR29536488	21W07152	Beijing	*10*
SRR29536501	21Z27162	Beijing	*10*
SRR29536498	21U09084	Beijing	*10*
SRR29536495	21R13433	Beijing	*10*
SRR29536492	21Z26414	Beijing	*10*
SRR29536489	21Z26733	Beijing	*10*
SRR29536502	21Z26354	Beijing	*10*
SRR29536499	21U09003	Beijing	*10*
SRR29536496	22U02252	Beijing	*10*
SRR29536493	21R13458	Beijing	*10*
SRR29536490	21R13603	Beijing	*10*

REFERENCES

1. Bolger AM, Lohse M, Usadel B. Trimmomatic: a flexible trimmer for Illumina sequence data. Bioinformatics 2014;30(15):2114 – 20. https://doi.org/10.1093/bioinformatics/btu170.
2. Li H, Durbin R. Fast and accurate long-read alignment with Burrows-Wheeler transform. Bioinformatics 2010;26(5):589 – 95. https://doi.org/10.1093/bioinformatics/btp698.
3. Li H, Handsaker B, Wysoker A, Fennell T, Ruan J, Homer N, et al. The sequence alignment/map format and SAMtools. Bioinformatics 2009;25(16):2078 – 9. https://doi.org/10.1093/bioinformatics/btp352.
4. McKenna A, Hanna M, Banks E, Sivachenko A, Cibulskis K, Kernytsky A, et al. The genome analysis toolkit: a MapReduce framework for analyzing next-generation DNA sequencing data. Genome Res 2010;20(9):1297 – 303. https://doi.org/10.1101/gr.107524.110.
5. Nguyen LT, Schmidt HA, von Haeseler A, Minh BQ. IQ-TREE: a fast and effective stochastic algorithm for estimating maximum-likelihood phylogenies. Mol Biol Evol 2015;32(1):268 – 74. https://doi.org/10.1093/molbev/msu300.
6. Wang XJ, Bing J, Zheng QS, Zhang FF, Liu JB, Yue HZ, et al. The first isolate of *Candida auris* in China: clinical and biological aspects. Emerg Microbes Infect 2018;7(1):93. https://doi.org/10.1038/s41426-018-0095-0.
7. Tse H, Tsang AKL, Chu YW, Tsang DNC. Draft genome sequences of 19 clinical isolates of *Candida auris* from Hong Kong. Microbiol Resour Announc 2021;10(1):e00308 – 20. https://doi.org/10.1128/mra.00308-20.
8. He H, Yang XM, Ma JH, Al-Danakh A, Pan SJ, Lin Y, et al. *Candida auris* infection; diagnosis, and resistance mechanism using high-throughput sequencing technology: a case report and literature review. Front Cell Infect Microbiol 2023;13:1211626. https://doi.org/10.3389/fcimb.2023.1211626.
9. Bing J, Du H, Guo PH, Hu TR, Xiao M, Lu S, et al. *Candida auris*-associated hospitalizations and outbreaks, China, 2018-2023. Emerg Microbes Infect 2024;13(1):2302843. https://doi.org/10.1080/22221751.2024.2302843.
10. Chen XF, Zhang H, Liu LL, Guo LN, Liu WJ, Liu YL, et al. Genome-wide analysis of in vivo-evolved *Candida auris* reveals multidrug-resistance mechanisms. Mycopathologia 2024;189(3):35. https://doi.org/10.1007/s11046-024-00832-7.

Methods and Applications

Application of an Integrated Risk Matrix and the Borda Count Method on Lassa Fever in Assessing the Importation Risk of EID — 9 African Countries, 1996–2023

Weijing Shang[1]; Yu Wu[1]; Jue Liu[1]; Wannian Liang[2]; Min Liu[1,#]

ABSTRACT

Introduction: Common methods for assessing and responding to outbreaks of emerging infectious diseases (EIDs) are usually applied in isolation and have limitations. This study aimed to integrate the risk matrix and Borda count methods to assess the importation risk of EIDs to China, using Lassa fever (LF) as an example.

Methods: This study used a mixed-methods approach combining multi-source data with an integrated risk matrix and Borda count method. Data were obtained from the World Health Organization, the Concise Statistics of International Students dataset, the United Nations World Tourism Organization, and the Statistical Yearbook. Importation risk was assessed across two dimensions: possibility and severity. Total importation risk was then categorized into 4 levels (low, moderate, high, and extremely high), corresponding to green, yellow, orange, and red zones, respectively, in the risk matrix assessment index. The Borda count method was used to rank the risks.

Results: The importation risk for 9 countries that experienced LF outbreaks from 1996 to 2023 was scored and ranked by importation possibility and severity to derive overall importation risks. This study determined that Nigeria posed the highest LF importation risk to China, ranking first among West African countries with the highest Borda points. Countries with moderate importation risk included Sierra Leone, Burkina Faso, and Ghana.

Discussion: An integrated risk matrix and Borda count method presented in this study may serve as a significant supplement to other risk assessment methods and enrich the current toolbox of public health countermeasures and inform future risk management of the importation of EIDs.

Under globalization, emerging infectious diseases (EIDs) can spread rapidly across countries and regions in a short time (*1*). Prioritization decisions for prevention and management are critical when facing potential outbreaks of EIDs. Responding to and controlling epidemics is costly due to limited resources and time. Risk assessment is the most common tool for assessing and responding to outbreaks of EIDs. It helps to identify risk factors, detect high-risk areas and possible spreaders, and enable health workers to take timely action to prevent and curb the spread of infectious disease.

Common risk assessment methods include expert consultation, Delphi, risk matrix, and analytical flowcharting. However, these methods have limitations (*2*). For example, the Delphi method requires complex preparation and consumes substantial time, human resources, and materials. Risk matrix is a decision support tool for visualizing and prioritizing risks (*3*). The Borda count method enables ranking risk events within the same risk level identified using a risk matrix (*4*–*5*). The integrated application of these two methods can guide resource allocation and has been used in diverse fields such as economics, medicine, engineering, business, and space operations (*3*,*6*). However, their application in assessing the importation risk of EIDs is limited.

In recent years, international cooperation for trade and personnel exchange between China and numerous countries has increased following the implementation of the "Belt and Road" initiative launched by China in 2013 (*4*,*7*). This increased interaction facilitates the cross-border transmission of EIDs. Lassa fever (LF) remains a substantial health concern in West Africa, presenting as an acute viral hemorrhagic illness with a high case fatality rate of 15%–30% (*8*–*9*). The virus transmits to humans through direct or indirect contact with infected rodents or contaminated materials (*8*). Severe infections manifest as respiratory distress, mucosal bleeding, hearing loss, and multiorgan failure. Generally, all populations are susceptible to LF (*8*).

Currently, no licensed vaccines or specific treatments are available (*8*). From 1996 to 2023, over 50 outbreaks of LF occurred in West Africa, with at least 18 imported cases of LF reported in several European countries (*1*). Notably, previously reported imported cases were primarily travelers and physicians diagnosed with LF after returning from epidemic areas (*1*). However, the importation risk of LF to China remains unclear. Therefore, this study used LF as an example to illustrate the application of risk matrix and Borda count method in assessing the risk of EIDs being imported to China.

METHODS

This study assessed the risk of EIDs importation using a mixed-methods approach, combining multi-source data with a risk matrix and Borda count method.

Data Acquisition

Data were obtained from the World Health Organization Disease Outbreak News (*1*), which includes the number of LF cases, deaths, imported cases, and fatality rates from 9 African countries from 1996 to 2023. Data on the annual number of African students in China were obtained from the 2018 Concise Statistics of International Students in China dataset (*10*). Data on the annual number of inbound and outbound tourists were obtained from the United Nations World Tourism Organization (*11*). Data on the number of persons sent for foreign economic cooperation, including the number of foreign contracted workers and personnel for labor service cooperation, were obtained from the China Statistical Yearbook 2019 (*12*) (Table 1).

MODEL FRAMEWORK

Risk Matrix Assessment

A risk matrix was applied to assess the risk of LF importation to China based on two dimensions: importation possibility and severity (Table 2) (*4*). Based on literature reviews (*8,13–14*), key indicators of these dimensions were identified. Importation possibility indicators included the time lag in years between the latest LF outbreak and 2024 and the number of cross-border migrants, including foreign students, tourists, labor workers, and other workers. Importation severity indicators included cumulative cases and the cumulative fatality rate. Scores for the risk assessment indicators were then determined in three steps. First, previous literature on infectious disease importation risk was reviewed (*4*). Second, the epidemiological characteristics of LF and the major populations undergoing cross-border mobility between China and Africa were summarized. Finally, expert consultation and discussion were conducted. Detailed information is shown in Table 3.

The formulas for importation possibility and

TABLE 1. Variables for the importation risk assessment of Lassa fever.

Country	Cumulative cases	Cumulative fatality rate (%)	The number of African students entering China	The number of African tourist arrivals to China by country	The number of persons sent by China to African countries for economic cooperations	The number of outbound Chinese tourist arrivals to African countries	The time lag between the latest outbreak of Lassa fever and 2024 by country (years)
Benin	125	24.00	634	4,503	917	10,233	8
Guinea	2	0	861	8,695	2,838	4,993	2
Liberia	39	41.03	802	3,832	2,954	NA	6
Nigeria	9,906	8.74	6,845	45,367	6,694	151,616	1
Sierra Leone	1,160	18.88	983	4,276	275	2,014	5
Togo	2	0	<500	4,517	83	6,490	2
Burkina Faso	1	100.00	<500	7,871	226	2,765	7
Ghana	14	7.14	6,475	22,890	963	7,917	1
Mali	2	0	788	4,868	422	4,671	7

Note: The number of African students entering China, the number of African tourist arrivals to China by country, the number of persons sent by China to African countries for economic cooperations, and the number of outbound tourists from China arriving in African countries: above data available were from the year of 2018; Cumulative cases and cumulative fatality rate (%) of Lassa fever are from the year of 1996–2023.
Abbreviation: NA=not appliable.

TABLE 2. Risk matrix assessment index.

Importation possibility	Importation severity				
	Negligible	Minor	Moderate	Severe	Catastrophic
Inevitable	H	H	E	E	E
Likely	M	H	H	E	E
Possible	L	M	H	E	E
Unlikely	L	L	M	H	E
Rare	L	L	M	H	H

Abbreviation: L=low importation risk; M=moderate importation risk; H=high importation risk; E=extremely high importation risk.

severity of LF are as follows. First, the importation possibility score was calculated as: the score of the time from the last outbreak to 2024 + (the score of the number of African students entering China × 30% + the score of the number of African tourist arrivals to China × 30% + the score of the number of persons sent for African economic cooperation × 20% + the score of the number of Chinese tourist arrivals to Africa × 20%). This study then derived the importation possibility risk score using 5 levels: rare (0–2 points); unlikely (3–4 points); possible (5–6 points); likely (7–8 points); and inevitable (9–10 points). The time lag in years between the latest outbreak of LF and 2024 was calculated by country as 2024 minus the outbreak year. Second, the importation severity score was calculated as the cumulative case score plus the cumulative fatality rate score. Cumulative cases were equal to the total number of cases in countries with LF from 1996 to 2023.

$$\text{Cumulative fatality rates} = \frac{\text{cumulative deaths from 1996 to 2023}}{\text{cumulative cases from 1996 to 2023}} \times 100\%$$

This study classified the final importation severity risk score into 5 levels: negligible (0–2 points); minor (3–4 points); moderate (5–6 points); severe (7–8 points); and catastrophic (9–10 points). Third, according to the importation possibility and severity levels in the risk matrix assessment index (Table 2), the importation risk of LF into China was divided into 4 levels (low, moderate, high, and extremely high), which corresponded to green, yellow, orange, and red zones, respectively. Finally, this study used the Borda count method to rank the LF importation risk (*4*).

Borda Count Method

This study used the Borda count method (*4*–*5*) to rank LF importation risks. First, the Borda points for each importation risk were calculated as the sum of the rank of its importation possibility and the rank of its severity risk level. This study then sorted the Borda points from largest to smallest and assigned corresponding counts of 0, 1,…, N-1. A lower Borda count indicates a greater likelihood of LF importation to China and potentially more severe consequences. Borda points were calculated using the following formula:

$$b_i = \sum_{k=1}^{m} (N - r_{ik})$$

Where N equals the total number of at-risk countries, this study defined at-risk countries as those with LF importation risk. Therefore, this study set N as 9. The variable m equals the 2 dimensions of risk assessment. r_{ik} equals the number of countries posing a higher risk than the risk for indicator i under criterion k, and b_i equals the Borda points of assessment indicator i.

RESULTS

This study scored and ranked the risk of LF importation from 9 countries that experienced LF outbreak from 1996 to 2023. It considered global importation possibility and severity to derive overall importation risks (Table 4). Using a risk matrix diagram, this study then visualized these total risks, with red, orange, yellow, and green representing extremely high, high, moderate, and low importation risk, respectively (Figure 1). Its integrated application of the risk matrix and Borda count method demonstrated that China faces a risk of LF importation. Regarding importation possibility, Nigeria presented the highest risk (score=8.7), while Mali presented the lowest (score 3.0). Concerning importation severity, Nigeria, Sierra Leone, and Burkina Faso exhibited the highest risk (score=6), whereas Mali had the lowest (score=2) (Table 4). Nigeria posed the highest LF importation risk (Figure

TABLE 3. Risk assessment indicators of importation possibility, severity, and corresponding scores.

Assessment indicators	Factors	Classification	Risk score
Importation possibility	The time lag between the latest outbreak of Lassa fever and 2024 by country (years)	≤1	5
		2–3	4
		4–5	3
		6–9	2
		≥10	1
	The number of African students entering China	≤999	1
		1,000–4,999	2
		5,000–9,999	3
		10,000–14,999	4
		≥15,000	5
	The number of African tourist arrivals to China by country	≤4,999	1
		5,000–9,999	2
		10,000–29,999	3
		30,000–49,999	4
		≥50,000	5
	The number of persons sent by China to African countries for economic cooperations	≤999	1
		1,000–2,999	2
		3,000–4,999	3
		5,000–9,999	4
		≥10,000	5
	The number of outbound Chinese tourist arrivals to African countries	≤4,999	1
		5,000–9,999	2
		10,000–49,999	3
		50,000–149,999	4
		≥150,000	5
Importation severity	Cumulative cases (cases)	≤49	1
		50–499	2
		500–999	3
		1,000–4,999	4
		≥5,000	5
	Cumulative fatality rate (%)	≤9	1
		10–29	2
		30–49	3
		50–69	4
		≥70	5

Note: The number of African students entering China, the number of African tourist arrivals to China by country, the number of persons sent by China to African countries for economic cooperations, and the number of outbound Chines tourist arrivals to African countries: above data available were from the year of 2018; Cumulative cases and cumulative fatality rate (%) of Lassa fever are from the year of 1996–2023.

1) due to the highest Borda points of 18 and ranking first. Sierra Leone, Burkina Faso, and Ghana presented moderate importation risks, while Guinea, Togo, Benin, Liberia, and Mali had low importation risks (Figure 1). Mali exhibited the lowest Borda points of 9 and ranked ninth (Table 4).

DISCUSSION

Risk assessment is foundational to preventing and containing the spread EIDs, and the risk matrix and Borda count method seem to be promising tools for

TABLE 4. Importation risks from countries with Lassa fever outbreaks to China from 1996–2023.

Country name	The importation possibility score	The importation severity score	Risk levels	Borda points	Borda count	Risk sequence of importation
Nigeria	8.7	6	H	18	0	1
Sierra Leone	4.0	6	M	14	1	2
Burkina Faso	3.3	6	M	14	2	2
Ghana	7.4	2	M	13	3	4
Guinea	5.5	2	L	11	4	5
Togo	5.2	2	L	11	5	5
Benin	3.4	4	L	11	6	7
Liberia	3.2	4	L	11	7	7
Mali	3.0	2	L	9	8	9

Abbreviation: L=low importation risk; M=moderate importation risk; H=high importation risk; E=extremely high importation risk.

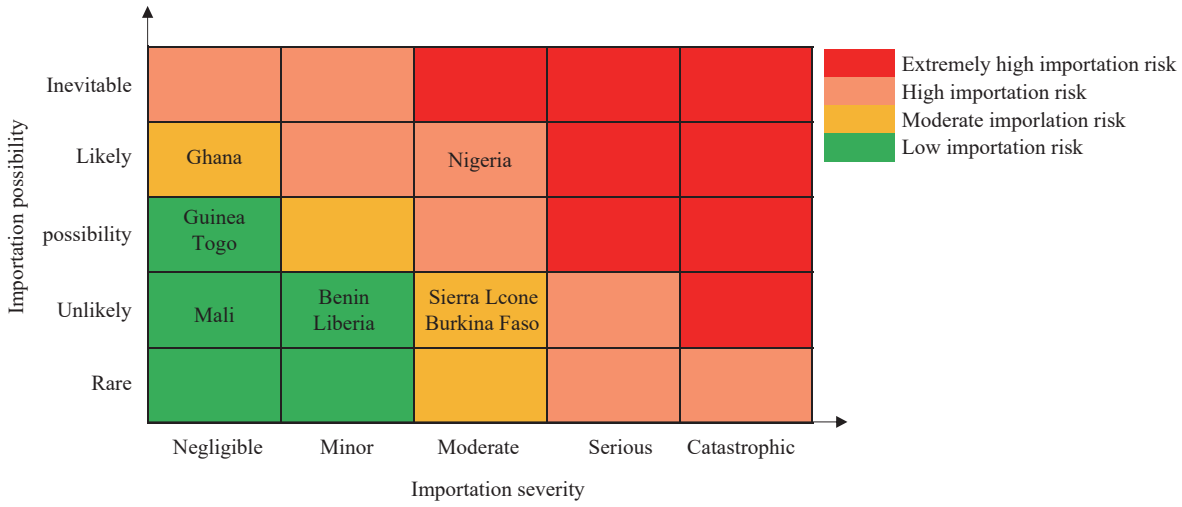

FIGURE 1. Importation risk of Lassa fever.

assessing the importation risk of a disease. This study attempted to assess the importation risk of EIDs to China, using LF as an example. Its authors believe that the method applied in this study may significantly supplement expert consultation and Delphi methods. Additionally, the method is more suitable for application in the early stages of a disease outbreak and offers advantages in assessing the potential risk of outbreaks under conditions of limited information and multi-source data.

This study leveraged multi-source data from multiple sectors, including tourism, international students, and cross-border labor, in addition to the health sector. Incorporating data such as flight information and the number of entrants from epidemic areas into the risk matrix could increase the accuracy of risk assessments. Furthermore, the effectiveness of the risk assessment hinges on the quality, timeliness, and type of multi-source data used; more comprehensive, timely, and accurate data sources yield more reliable results.

In this study, it was found that Nigeria presented a high risk of LF importation to China, with moderate importation severity and likely importation possibility. Currently, the LF epidemic status in Nigeria is worrisome. A significant increase in the number of suspected and confirmed LF cases was reported in Nigeria from 2021 to 2023 (*1*,*14*). LF infection rates exhibited seasonal variability in Nigeria, with significantly higher rates in the dry season than in the wet season (*15*). During the dry season, human activities such as bush burning are commonly practiced in the Forest and Savannah regions to hunt rodents, including *Mastomys natalensis*, for food (*15*). *Mastomys natalensis*, a natural host of Lassa virus, has a high reproductive rate in West Africa and plays a significant role in rodent-to-human transmission of the virus (*8*,*15*). Bush burning destroys rodent habitats,

encouraging their movement from bushes to human dwellings in search of shelter and food, which may increase the risk of LF exposure for humans (*15*). Other factors, including nosocomial transmission, travel and migration, inadequate public health infrastructure, the effects of civil war and conflict, and social factors may also contribute to the re-emergence of LF epidemics in Nigeria (*14*). Additionally, among nine countries, Nigeria has the largest number of entrants to China, including international students and tourists. China has also sent a large number of workers to Nigeria for economic cooperation projects, and many Chinese tourists travel to Nigeria. Globalization and the implementation of China's "Belt and Road" strategy will likely lead to a significant increase in the volume and speed of travel between the two countries (*4*,*7*). Consequently, the cross-border spread of LF is facilitated.

In this study, the risk matrix and Borda count method were applied to assess the importation risk of LF to China and distinguish risk levels. High-risk importation areas can thus be quickly identified. These results facilitate the government to make plans, allocate limited resources, and develop preventive strategies for LF. Furthermore, the risk matrix and Borda count method may be used to assess and rank the risk of various imported EIDs with descending order of risk. This ranking can then inform the determination of the disease with the highest risk. The final risk assessment results may provide evidence for China to develop and optimize preparedness strategies, improve the efficiency of risk management and infectious disease prevention, and help prevent or curb future outbreaks. Currently, the Chinese Center for Disease Control and Prevention has established a risk assessment group (*16*). This group uses expert consultation to assess the risk of public health emergencies that may occur in or be imported from abroad each month (*16*). Finally, the integrated application of the risk matrix and Borda count method presented in this study may enrich the current toolbox of public health countermeasures and inform future risk management of imported EIDs.

This study has some limitations. First, while this study introduced the integrated risk matrix and Borda count method, other methods exist but were not included. Additionally, expert consultation and Delphi methods should be employed to assess the importation risk of EIDs more comprehensively. Second, this study focused on LF importation risk for the entire Chinese population. Due to the unavailability of cross-national data for the whole population, the populations used to assess LF importation risk — students, tourists, businesspeople, and laborers — were primarily young and middle-aged adults. Compared with the whole population, these groups may have a lower LF importation risk due to better hygiene knowledge and protection awareness, stronger immunity, and a lower LF infection risk. Therefore, the actual levels in this study may be underestimated. Finally, the risk matrix relies on multi-source data; the wider and more accurate the data sources, the better the model's application. This study used LF, a skin-to-skin contact infection, as an example. The risk matrix and Borda count method can also be applied to the importation risk assessment of vector-borne diseases and infectious diseases with other transmission types. For example, assessing malaria would require data on the host, medium, climate, and environment.

Conflicts of interest: No conflicts of interest.

Funding: Supported by the grant from the National Natural Science Foundation of China (71934002), and National Key Research and Development Project of China (2021ZD0114104).

doi: 10.46234/ccdcw2024.234

[#] Corresponding author: Min Liu, liumin@bjmu.edu.cn.

[1] School of Public Health, Peking University, Beijing, China; [2] Vanke School of Public Health, Tsinghua University, Beijing, China.

Submitted: July 15, 2024; Accepted: October 02, 2024

REFERENCES

1. World Health Organization. Emergencies—disease outbreak news (DONs). 2024. https://www.who.int/emergencies/disease-outbreak-news. [2024-5-11].
2. Chinese Center for Disease Control and Prevention. Technical program for public health risk assessment of emergencies (trial). 2017. https://www.chinacdc.cn/jkzt/tfggwssj/gl/201708/t20170810_149318.html. [2024-6-4]. (In Chinese).
3. Kaya GK, Ward J, Clarkson J. A review of risk matrices used in acute hospitals in England. Risk Anal 2019;39(5):1060 – 70. https://doi.org/10.1111/risa.13221.
4. Shang WJ, Jing WZ, Liu J, Liu M. Global epidemic of ebola virus disease and the importation risk into China: an assessment based on the risk matrix method. Biomed Environ Sci 2023;36(1):86 – 93. https://doi.org/10.3967/bes2023.008.
5. Zhang YP. Public health risk assessment of Hankou river beach park during the 7th CISM Military World Games [dissertation]. Wuhan: Wuhan University; 2020. http://dx.doi.org/10.27379/d.cnki.gwhdu.2020.000510. (In Chinese).
6. Gray G, Bron D, Davenport ED, d'Arcy J, Guettler N, Manen O, et al. Assessing aeromedical risk: a three-dimensional risk matrix approach. Heart 2019;105(Suppl 1):s9 – 16. https://doi.org/10.1136/heartjnl-2018-313052.
7. Liu J, Liu M. Focus on epidemics of infectious diseases, prevention of risk of cross-border transmission. Chin J Epidemiol 2022;43(7):1049 – 52. https://doi.org/10.3760/cma.j.cn112338-20220125-00073.
8. World Health Organization. Lassa fever. 2017. https://www.who.int/

news-room/fact-sheets/detail/lassa-fever. [2024-5-10].
9. Erameh CO, Koch T, Edeawe OI, Oestereich L, Omansen T, Jochum J, et al. Focussed Assessment with Sonography in acute Lassa Fever (FASLa): development of a point-of-care protocol and description of common ultrasound findings. J Infect 2023;87(1):27 – 33. https://doi.org/10.1016/j.jinf.2023.04.008.
10. Ministry of Education, Department of International Cooperation and Exchange. Concise statistics of international students in 2018. Ministry of Education, Department of International Cooperation and Exchange. 2018.
11. United Nations World Tourism Organization. Tourism statistics. https://www.e-unwto.org/toc/unwtotfb/current. [2024-6-1].
12. National Bureau of Statistics of China. China statistical yearbook 2019: 17-13 foreign inbound tourists by country. China Statistics Press, 2019. [2024-6-1]. https://www.stats.gov.cn/sj/ndsj/2019/indexch.htm. (In Chinese).
13. Garry RF. Lassa fever - the road ahead. Nat Rev Microbiol 2023;21(2):87 – 96. https://doi.org/10.1038/s41579-022-00789-8.
14. Malik S, Bora J, Dhasmana A, Kishore S, Nag S, Preetam S, et al. An update on current understanding of the epidemiology and management of the re-emerging endemic Lassa fever outbreaks. Int J Surg 2023;109(3):584 – 6. https://doi.org/10.1097/JS9.0000000000000178.
15. Yaro CA, Kogi E, Opara KN, Batiha GES, Baty RS, Albrakati A, et al. Infection pattern, case fatality rate and spread of Lassa virus in Nigeria. BMC Infect Dis 2021;21(1):149. https://doi.org/10.1186/s12879-021-05837-x.
16. Du MX, Li Y, Zhao HT, Liu FF, Huang XX, Li MS, et al. Risk assessment of public health emergencies concerned in China, April 2024. Dis Surveil 2024;39(4):395 – 7. https://doi.org/10.3784/jbjc.202404220250.

Recollection

Retrospective Analysis of the Epidemiological Evolution of Brucellosis in Animals — China, 1951–1989 and 1996–2021

Zhiguo Liu[1]; Miao Wang[2]; Yingqi Wang[3]; Min Yuan[1]; Zhenjun Li[1,4,#]

ABSTRACT

Brucellosis poses a significant threat to public health in China. This study utilized a range of epidemiological indices, including seroprevalence and the number of reported cases, to illustrate the epidemic profile of the disease. Although the seroprevalence of brucellosis in animals (including sheep, goats, cattle, and swine) steadily decreased from a severe epidemic level in the 1950s to a low endemic level by 1989, the disease reemerged in 2000. Subsequently, there has been a persistent increase in the frequency of outbreaks and the number of reported cases from 2006 to 2021, with over 98% of reported cases occurring in sheep and cattle. During this period, the culling rate declined, while infection rates increased, nearly reversing their respective trajectories. The decrease in the culling rate of positive animals coincided with an increase in infection rates, indicating that infection among these animals was persistent and circulating. In the southern regions of China, 6.34% (34,070 of 537,797) of cases were reported between 2006 and 2021, whereas in the northern regions, 93.67% (503,727 of 537,797) of cases occurred during the same timeframe. Each time cases increased in the south, they lagged 2 to 5 years behind those in the north, suggesting that stringent control measures for sheep and cattle in the north should be prioritized. These findings provide critical insights into developing control strategies to mitigate the spread of the disease.

Brucellosis is a zoonotic disease that threatens livestock economies in many low-income countries, causing considerable economic losses due to animal abortions and reduced productivity (*1*–*2*). In 1887, David Bruce first isolated *B. melitensis* from the spleens of four deceased soldiers on Malta Island who had consumed raw goat milk (*3*). In the past 136 years, brucellosis has become a globally spread zoonotic disease present on all 6 continents, especially in Asia and Africa, which harbor the highest disease burden. This poses a severe public health risk to farmers and animal owners (*4*–*5*). *Brucella* spp. invade the genital systems of animals, leading to abortion or stillbirth at the end of pregnancy, and present with epididymitis or orchitis, affecting the productive capacity of male animals (*6*). Infected animals and their products are the main source of infection in humans. Currently, brucellosis is still expanding in low-income countries due to many socioeconomic factors, including international trade, immigration, travel to endemic areas, and the developing breeding industry aimed at increasing the income of farmers, including those in China (*7*–*8*).

Brucellosis, a significant public health concern in China, has a long history marked by an initial animal epidemic documented in 1936 (*9*). This first epidemic, spanning from 1950 to 1984, was followed by a period of declining infection rates, nearly reaching China's control standards between 1985 and 1995. However, as an emerging infectious disease, brucellosis has reemerged with cases reported across 31 provincial-level administrative divisions (PLADs) in the Chinese mainland (*10*). Growth of the livestock industry, particularly in sheep and goat farming, coupled with economic development, has contributed to frequent animal brucellosis outbreaks in numerous PLADs from 2006 to 2021 (*11*). Retrospective analysis of both epidemic stages is crucial to understand the epidemiological evolution of animal brucellosis. This study aims to investigate these epidemic trends in China and define the regional distribution of circulating *Brucella* strains across different periods, providing insights for targeted brucellosis control measures.

METHODS

Data Source, Processing, Analysis, and Visualization

In this study, surveillance data from two epidemic

phases (I: 1951–1989 and II: 2006–2021) of brucellosis in animals were collected and analyzed to illustrate the epidemiological profile. Epidemic data on animal brucellosis were collected from the *Annals of Animal Diseases in China* (1951–1989) and the *Official Veterinary Bulletin* (2006–2021). The seroprevalence of animal brucellosis and the number and biotypes of *Brucella* strains in different PLADs were extracted from *Animal Diseases in China* (1952–1989). Five epidemic items were extracted from the *Official Veterinary Bulletin* [2006–2021 (September), http://www.agri.gov.cn]: 1) the total number of outbreaks each month, 2) number of cases each month, 3) animal species (hosts), 4) number of animal deaths each month, and 5) number of animals destroyed each month. Excel 2016 (Microsoft, Redmond, WA, USA) was used for data curation, processing, analysis, and visualization. A semi-logarithmic curve was used to depicte the changing trends in the positive case rates and the culling rates. OmicShare tools (*12*) (https://www.omicshare.com/tools/) were used for Pearson correlation analysis of the incidence of human brucellosis, the infected rates, and the livestock breeding situation.

RESULTS

Sheep and Goat Brucellosis Seroprevalence from 1951 to 1989

From 1951 to 1989, the seroprevalence of sheep brucellosis among 15 PLADs was 1.84% (993,609/54,068,364). The highest positive rate was 5.92% (520,140/8,788,690) in the 1960s (1960–1969), followed by 3.58% (234,154/6,543,382) in the 1950s (1951–1959), 2.18% in the 1970s (1970–1979), and 0.3% (95,582/32,129,518) in the 1980s (1980–1989) (Table 1). Sheep brucellosis was widespread from 1951 to 1959. The seroprevalence in Qinghai Province was 6.58% (16,280/247,365) from 1950 to 1959; in Heilongjiang Province was 8.5% from 1956 to 1958; and in Xinjiang Uygur Autonomous Region was 9.19% from 1956 to 1964. Sheep brucellosis was severe from 1961 to 1969, with seropositive rates in Qinghai and Xinjiang PLADs from 1960 to 1969 at 12.78% (16,280/247,365) and 4.16% (202,488/4,870,090), respectively. In Ningxia Hui Autonomous Region, the rate was 11.3% from 1963 to 1966.

Sheep brucellosis seroprevalence declined from 1970 to 1979. However, some regions remained heavily affected, with 9.26% seroprevalence in Qinghai Province and 3.98% in Xinjiang Uygur Autonomous Region. From 1980 to 1989, sheep brucellosis was gradually controlled in some initially high-epidemic regions. Seroprevalence decreased in Shaanxi, Gansu, Ningxia, Xizang, Jilin, Liaoning, and Qinghai PLADs. In Qinghai Province, the positive rate decreased from 9.26% in the 1970s to 3.06% in the 1980s, while in Gansu Province, it decreased from 4.66% in 1981 to 0.10% in 1986, and the positive rate decreased from 2.54% in the 1950s to 0.54% in the 1980s. Positive rate in Xinjiang Uygur Autonomous Region declined to 0.79% in the 1980s. From 1987 to 1989, the overall sheep seroprevalence in 30 PLADs (excluding Chongqing Municipality) was 0.59% (6,113/

TABLE 1. Seroprevalence of brucellosis in sheep/goats, cattle/cows, and swine from the 1950s to the 1980s.

Hosts	Numbers/cases/rate	1951–1959	1960–1969	1970–1979	1980–1989	Total
Sheep/goats	Tested number (heads)	6,543,382	8,788,690	6,606,774	32,129,518	54,068,364
	Positive cases (heads)	234,154	520,140	143,733	95,582	993,609
	Positive rate (%)	3.58	5.92	2.18	0.30	1.84
Bovine	Tested number (heads)	1,289,667	3,703,368	7,773,531	9,589,551	22,356,117
	Positive cases (heads)	59,701	110,020	89,214	53,197	312,132
	Positive rate (%)	4.63	2.97	1.15	0.55	1.40
Swine	Tested number (heads)	2,149	6,714	20,783	285,979	315,625
	Positive cases (heads)	524	687	906	9,566	11,683
	Positive rate (%)	24.83	10.23	4.36	3.35	3.70

Note: Tested data in sheep were from 15 PLADs, including Tianjin, Inner Mongolia, Hebei, Jilin, Heilongjiang, Shandong, Yunnan, Shaanxi, Gansu, Zhejiang, Qinghai, Ningxia, and Xinjiang. Tested data in cattle/cows were from 22 PLADs from 1952 to 1989, including Tianjin, Inner Mongolia, Hebei, Jilin, Heilongjiang, Liaoning, Hubei, Beijing, Jiangsu, Anhui, Fujian, Henan, Guangdong, Sichuan, Shandong, Yunnan, Shaanxi, Gansu, Zhejiang, Qinghai, Ningxia, and Xinjiang. Tested data in swine were from 11 PLADs from 1955 to 1989, including Tianjin, Hebei, Liaoning, Zhejiang, Hunan, Guangdong, Yunnan, Shaanxi, Gansu, Xinjiang, and Inner Mongolia.
Abbreviation: PLADs=provincial-level administrative divisions.

1,037,181), ranging from 0.10% (Jilin Province) to 7.44% (Jiangsu Province) (Table 2).

Bovine (Cattle) Brucellosis Seroprevalence from 1951 to 1989

The overall seroprevalence of brucellosis in cattle from 22 PLADs was 1.4% (312,132/22,316,117) from 1952 to 1989. The seroprevalence in cattle gradually declined from 4.63% (59,701/1,289,667) from 1952 to 1959, to 2.97% (110,020/3,703,368) from 1960 to 1969, to 1.15% (89,214/7,733,531) from 1970 to 1979, and to 0.55% (53,197/9,589,551) from 1980 to 1989. In the 1950s, brucellosis in cattle was common in the north. The infection rates were 46.43%, 19.3%, 11.57%, and 12.27% in Ningxia, Qinghai, Gansu, and Xinjiang PLADs, respectively. Subsequently, the seroprevalence in cattle gradually declined from the 1950s to the 1980s, with rates of 1.60% in Xinjiang,

TABLE 2. Seroprevalences in brucellosis of sheep/goats, cattle/cows, and swine from 1987 to 1989.

PLADs	Sheep/goats (heads)			Cattle/cow (heads)			Swine (heads)		
	Tested number	Number of positive cases	Positive rate (%)	Tested number	Number of positive cases	Positive rate (%)	Tested number	Number of positive cases	Positive rate (%)
Beijing	17,446	6	0.03	12,909	12	0.09	1,754	5	0.29
Tianjin	1,592	0	0	1,013	0	0	2,254	0	0
Hebei	22,791	130	0.57	4,474	64	1.43	25	0	0
Shanxi	13,446	312	2.32	4,185	35	0.84	3,548	12	0.38
Inner Mongolia	118,400	296	0.25	10,807	118	1.09	884	26	2.14
Liaoning	63,964	322	0.50	52,730	447	0.80	3,819	14	0.30
Jilin	46,434	5	0.01	32,733	48	0.15	0	0	0
Heilongjiang	246,946	461	0.19	288,841	1,683	0.56	9,879	40	0.14
Shanghai	949	0	0	52,135	8	0.02	152,613	407	0.27
Jiangsu	1,666	124	7.44	8,237	28	0.34	3,417	69	2.19
Zhejiang	13,975	11	0.08	36,328	53	0.15	15,388	3	0.02
Anhui	1,687	31	1.84	2,662	15	0.60	1,146	32	2.80
Fujian	8,051	28	0.35	15,961	170	1.07	10,228	154	1.51
Jiangxi	328	0	0	4,181	1	0.17	4,301	6	0.14
Shangdong	31,390	225	0.81	21,016	97	0.46	0	0	0
Henan	3,635	26	0.71	5,854	57	0.97	6,585	2	0.03
Hubei	5,448	93	1.71	9,577	165	1.72	10,043	249	2.48
Hunan	4,169	115	2.76	12,396	423	3.41	11,910	483	4.06
Guandong	0	0	0	8,442	2	0.02	27,788	443	1.59
Guangxi	781	1	0.12	3,671	4	0.11	4,385	56	1.27
Hainan	60	0	0	1,249	8	0.64	858	7	6.82
Sichuan	109,609	2,036	1.86	30,017	498	1.66	16,256	107	0.66
Guizhou	2,407	14	0.58	3,733	86	2.30	2,684	30	1.18
Yunnan	5,775	19	0.33	8,327	1	0.01	7,878	8	0.10
Xizang	0	0	0	10,975	262	2.38	0	0	0
Shaanxi	31,545	92	0.29	8,085	24	0.39	3,069	12	0.39
Gansu	14,439	30	0.20	11,748	56	0.47	1,500	0	0
Qinghai	43,506	343	0.79	5,175	503	9.72	1,733	55	3.17
Ningxia	76,337	524	0.69	23,625	118	0.59	1,090	28	2.57
Xinjiang	150,405	869	0.58	114,691	735	0.64	5,359	52	0.97

Abbreviation: PLADs=provincial-level administrative divisions.

1.05% in Ningxia, and 8.9% in Qinghai in the 1980s. Epidemics and outbreaks gradually decreased and were controlled in regions with high seroprevalence. Brucellosis was still endemic in some previously low-epidemic regions from 1980 to 1984, at rates of 7.22% in Jiangxi, 6.66% in Liaoning, 5.20% in Hubei, 4.53% in Henan, 3.52% in Hunan, and 2.30% in Guizhou. Finally, the overall seroprevalence in cattle in all 30 PLADs (except Chongqing) decreased to 0.71% (5,727/803,782), with the lowest being 0.02% in Guangdong and the highest being 3.41% in Hunan Province.

Brucellosis Seroprevalence in Swine and Dogs from 1951 to 1989

Swine brucellosis seroprevalence was 3.7% (11,683/315,443) in 11 PLADs from 1955 to 1989, with rates of 24.38% (524/2,149) in the 1950s, 10.23% (687/6,714) in the 1960s, 4.36% (906/20,783) in the 1970s, and 3.35% (9,565/285,797) in the 1980s. Before the 1980s, swine brucellosis was atypical but locally endemic in Guangxi and Guangdong, where breeding swine production was prominent. In 1952, the Guilin Liangfeng swine farm in Guangxi introduced four Berkshire breeding pigs from Hong Kong Special Administrative Region (SAR), China, resulting in numerous infections and swine abortions. The seroprevalence in Guangxi in 1952 was 51.5% (381/739). In 1980, the swine brucellosis seroprevalence increased, peaking in 1985 at 8.15%, and subsequently declined continuously to 0.74% (2,300/310,394) from 1987 to 1989. Rates were 0.03% (2/6,585) in Henan and 4.06% (483/11,910) in Hunan (Table 2). In the late 1980s, *Brucella canis* brucellosis was reported, and *B. canis* was isolated and identified. The average positivity rate in 8 PLADs was 6.72% (141/2,099). Dog seroprevalence was 14.74% in Xinjiang from 1965 to 1989 and 22.5% in Qinghai. Seroprevalence in horses, deer, camels, poultry, and wildlife, such as yaks, has also been reported (*13*).

Animal Brucellosis Outbreaks from 2006 to 2021

From 2006 to 2021, a total of 38,248 outbreak events were recorded. The number of outbreaks increased from 90 in 2006 to a maximum of 6,126 in 2011 and then declined to 3,133 in 2021 (Figure 1A). Outbreak events were observed each month, with 62.19% (23,787/38,248) recorded from June to October. Most outbreaks occurred in August (5,418), followed by September (*n*=5,181), July (*n*=4,710), and June (*n*=4,291), with the fewest occurring in February (*n*=794) (Figure 1B). The average number of reported outbreak events was 2,390.5 per year and 3,187.3 per month. Sheep and cattle accounted for approximately 99.2% of cases, with 218,168 in sheep, 11,625 in cattle, and 303,609 in both. The proportion of cases involving other animal species was low. Additionally, 1,759 cases included deaths caused by *Brucella* infection, accounting for 0.33% of deaths in Inner Mongolia, Shaanxi, and Xinjiang.

Time and Seasonal Distribution Profiles of Animal Cases From 2006 to 2021

Between 2006 and 2021, a total of 537,797 cases were reported. The number of cases was 2,031 in 2006, rapidly increased to 125,030 in 2011, and then declined to 59,494 in 2020. The lowest number of cases (*n*=1,280) was observed in 2007 (Figure 2A). Although the number of cases fluctuated and decreased after the 2011 peak, there were at least five times more cases in 2021 than in 2006. The range of case counts across months was 10,233–65,480, with 54.1% of cases reported from April to September. Most cases occurred in June, followed by August (*n*=54,828) and July (*n*=48,792), with the lowest number occurring in January (Figure 2B).

Geographic Distribution of Animal Cases, 2006–2021

Animal brucellosis outbreaks were reported in 28 PLADs from 2006 to 2021, excluding Tianjin, Hainan, and Xizang PLADs. Inner Mongolia reported the highest number of outbreaks (21,860) between 2006 and 2021 (Figure 3), with a dramatic increase from 215 in 2010 to 5,464 in 2011, followed by a decline to 609 in 2021. Xinjiang reported 8,985 cases during the study period, with the number of outbreaks gradually increasing annually from 2 in 2006 to 1,543 in 2021. A similar trend was observed in Shaanxi Province, with outbreaks gradually increasing from 3 in 2006 to 744 in 2021. In the south, Hubei (*n*=931) and Zhejiang (*n*=518) reported the most outbreaks, both exhibiting an initial increasing trend followed by a gradual annual decline. The fewest cases were reported in Anhui (*n*=11), followed by Sichuan (*n*=24), Beijing (*n*=39), Shanghai (*n*=43), Guangxi (*n*=52),

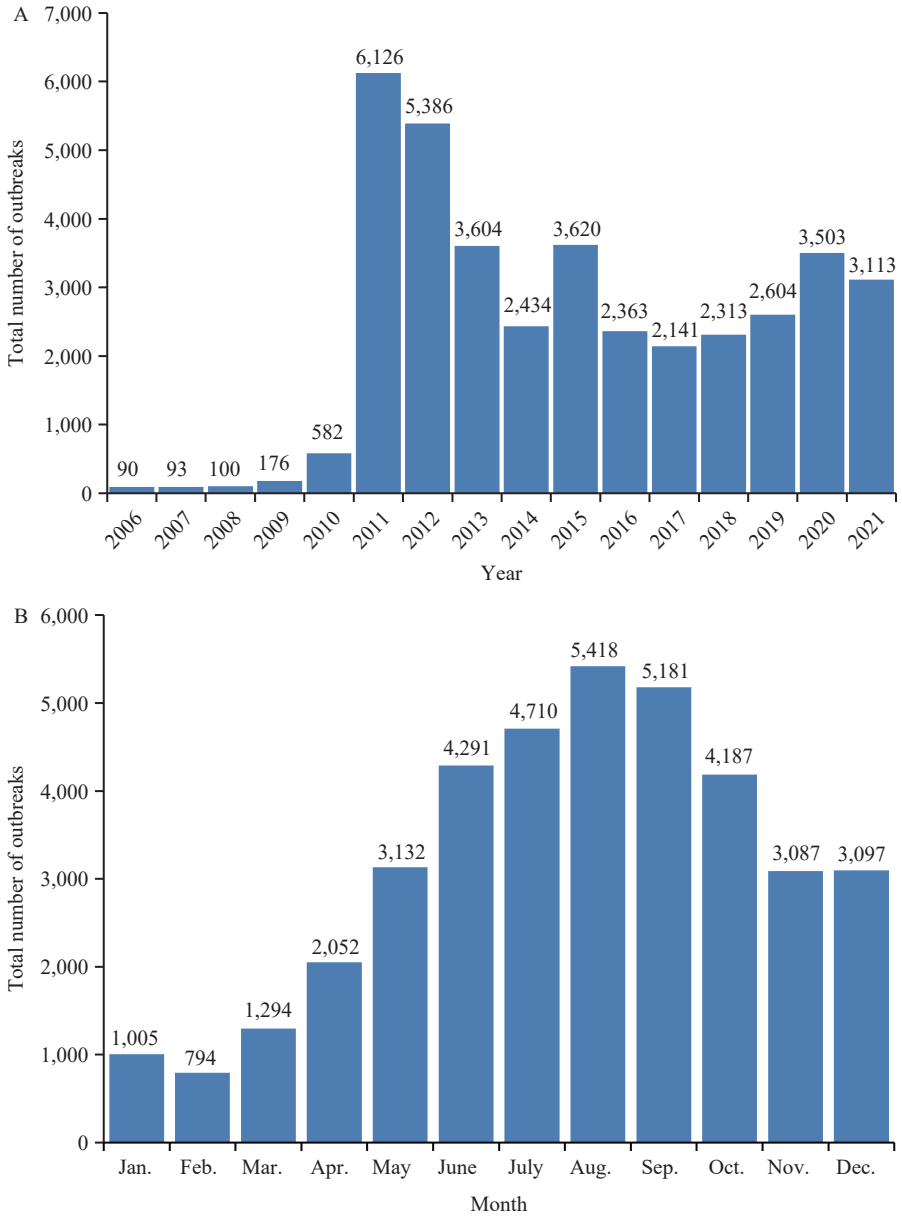

FIGURE 1. Brucellosis outbreak event in animals from 2006 to 2021. (A) Total number; (B) Seasonal distribution profile.
Note: Total outbreak number of brucellosis included the outbreak events from bovine, sheep, goats, and other hosts in this period.

Ningxia (*n*=57), and Guangdong (*n*=59). Other regions reported between 60 and 454 outbreaks. Approximately 40% of outbreaks occurred from 2011 to 2013, with 6,136 in 2011, 5,346 in 2012, and 3,604 in 2013. A total of 537,797 animal cases tested positive across 28 PLADs. Of these, 6.34% (34,070/537,797) were in the south and 93.67% (503,727/537,797) were in the north (Figure 4). Most cases were reported in Inner Mongolia (*n*=346,785), Xinjiang (*n*=105,367), and Shanxi (*n*=23,399), while Beijing reported the fewest (*n*=171). In the north, cases continuously increased from 1,797 in 2006 to 58,369 in 2020 before declining to 18,419 in 2021. In the south, Hubei reported the most cases (*n*=10,839), followed by Yunnan (*n*=5,888), Henan (*n*=4,841), and Zhejiang (*n*=4,536). Conversely, Sichuan recorded the lowest number (*n*=91). Southern cases rose from 234 in 2006, peaked in 2016 (*n*=8,014), and then fluctuated before declining to 741 in 2021. Notably, cases in the south increased with a lag of two to five years compared to the north. The peak occurred in the north in 2011 and in the south in 2016 (Figure 4).

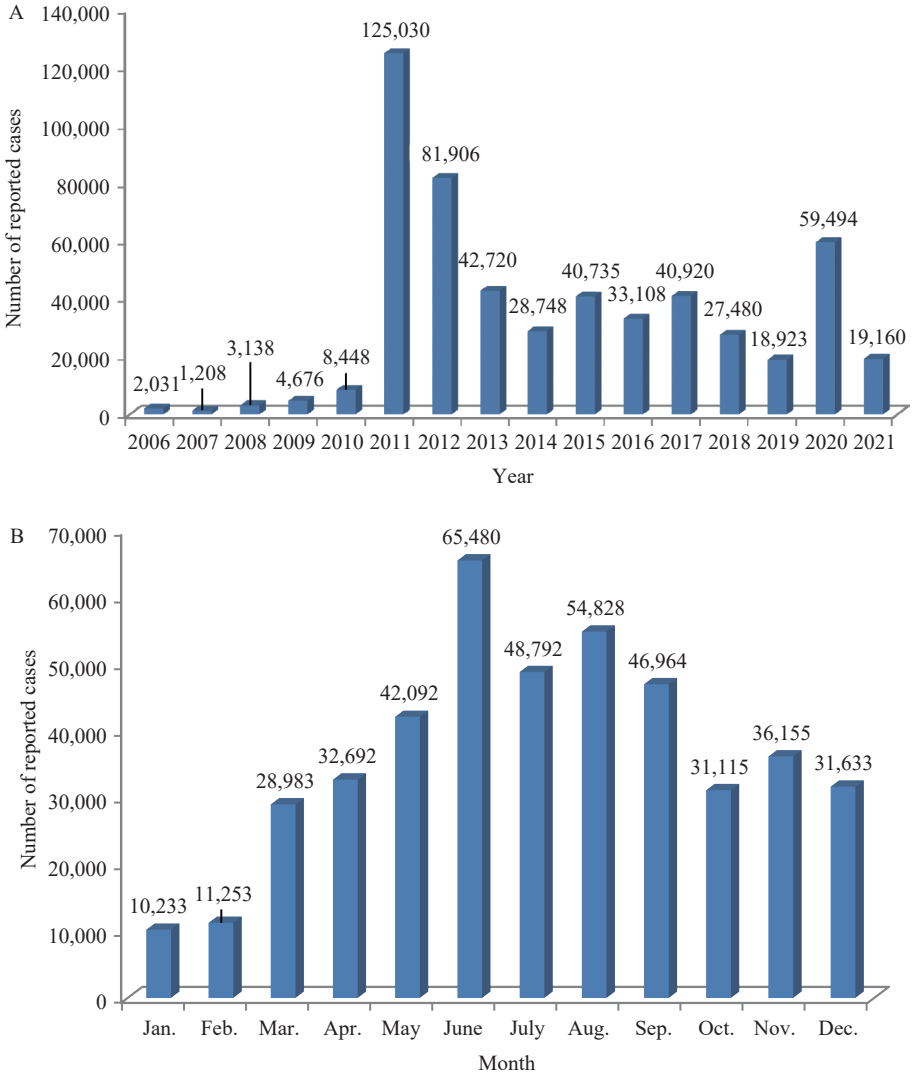

FIGURE 2. Reported brucellosis cases in animals from 2006 to 2021. (A) Total number; (B) Seasonal distribution profile.
Note: The total number of reported animal brucellosis cases included cases reported from bovine, sheep, goats, and other hosts in this period.

Time and Geographic Profile of Culled-Positive Animals from 2006 to 2021

The total culling rate of positive animals was 70.14% (377,230/537,797). The culling rate gradually declined from 103.3% in 2006 to 4.32% in 2017 and then fluctuated between 40.4% and 109.3% from 2017 to 2021 (Figure 5A). The trends in culling and infection rates between 2006 and 2021 were almost reversed. The culling rate of positive animals declined with an increase in the infection rate (Figure 5B). These data provide irrefutable evidence that the source of brucellosis infection is persistent and may move between herds and regions. Sichuan Province had the highest culling rate of positive animals (170.33%), followed by Anhui (157.29%), Beijing (156.73%), and Guangxi (155.35%) (Figure 5A). Additionally, the culling rates in nine PLADs were above 100%: Fujian, Shanghai, Jiangxi, Guangdong, Jiangsu, Jilin, Yunnan, Heilongjiang, and Guizhou (Figure 5A). However, the culling rates in 15 others PLADs were below 100%, with the lowest culling rate in Hubei [61.75% (6,693/10,839)], followed by 66.70% in Xinjiang, 68.98% in Ningxia, 70.77% in Shanxi, 78.26% in Shandong, 84.32% in Liaoning, and 84.69% in Inner Mongolia (Figure 5A). Furthermore, correlation analysis showed that the number of sheep and the infection rate of animal brucellosis were significantly correlated with the incidence rate and number of human brucellosis cases ($P \leq 0.001$) (Figure 6).

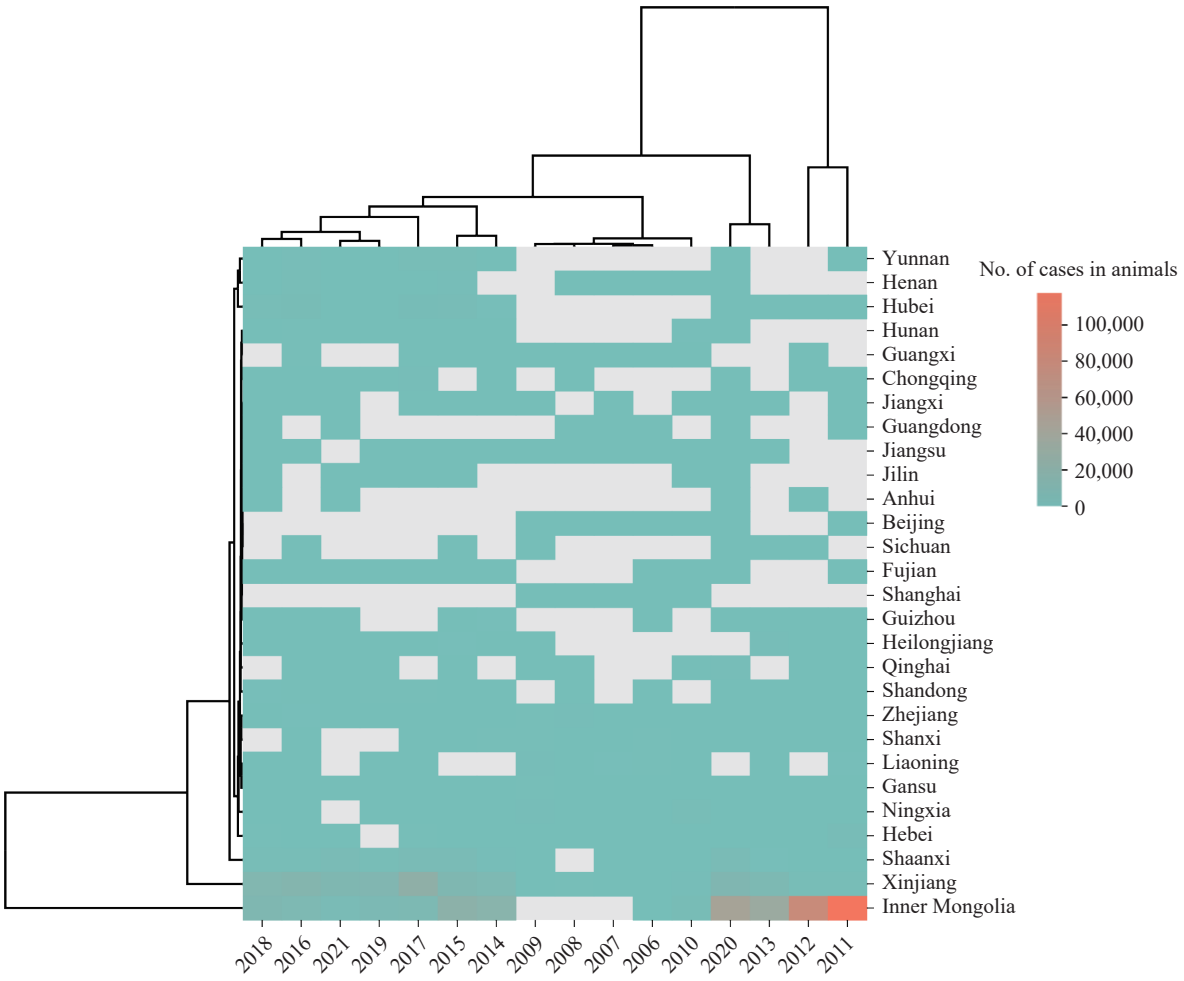

FIGURE 3. The distribution of reported brucellosis cases in animals at the PLADs level from 2006 to 2021.
Note: Number of cases reported in each province included those from bovine, sheep, goats, and other hosts in this period.
Abbreviation: PLADs=provincial-level administrative divisions.

District-Level Distribution of *Brucella* Species/Biovars

From 1951 to 1989, 2,015 *Brucella* strains were collected from animals, including 1,523 *B. melitensis* strains, 250 *B. abortus* strains, 208 *B. suis* strains, 32 *B. canis* strains, and 2 *B. ovis* strains. During this period, *B. melitensis* was mainly found in Xinjiang (*n*=286), followed by Shaanxi (*n*=217), Jilin (*n*=207), Henan (*n*=109), Sichuan (*n*=25), and fewer strains in Guangxi, Yunnan, and Fujian PLADs. *B. abortus* strains were dominant in Sichuan (*n*=122), Xinjiang (*n*=56), and Jilin (*n*=30). *B. suis* strains were distributed in Guangxi (*n*=98) and Guangdong (*n*=90). Fewer *B. canis* strains were observed in Sichuan, Fujian, Guangdong, and Guangxi PLADs (Supplementary Table S1, available at https://weekly.chinacdc.cn/). Additionally, only two *B. ovis* strains were isolated from Urumqi, Xinjiang. However, from 1996 to 2021, only 303 *Brucella* strains were isolated and identified from animals, with 254 *B. melitensis*, 26 *B. abortus*, and 23 *B. suis* strains. During this period, most *B. melitensis* strains were found in Xinjiang (*n*=101), Inner Mongolia (*n*=78), and Gansu (*n*=26). *B. abortus* strains were distributed in Hebei (*n*=11), Heilongjiang (*n*=10), and Xinjiang (*n*=5) PLADs. Additionally, 22 *B. suis* strains were isolated from animals in Inner Mongolia. The number and diversity of species/biotypes have gradually decreased, indicating a significant difference between the current serious epidemic situation of brucellosis and the number of strains in humans. Furthermore, the species/biotype distribution pattern of *Brucella* showed a pronounced shift from multiple co-driven species before the 2000s to a single dominant species, *B. melitensis*, after the 2000s.

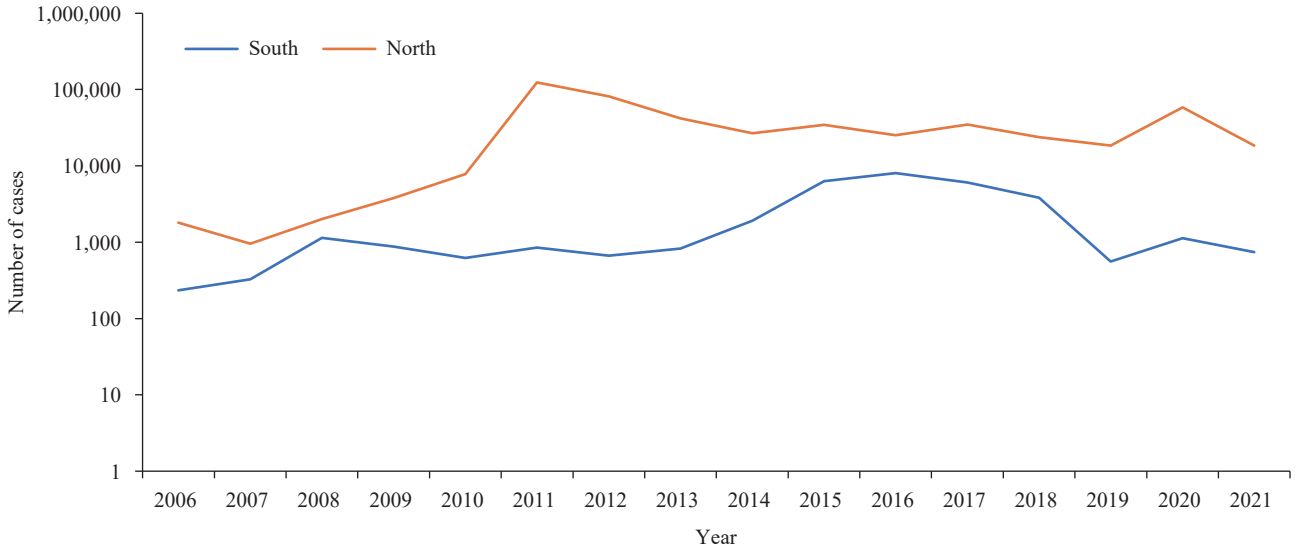

FIGURE 4. Distribution profile of reported brucellosis cases in animals between southern and northern regions from 2006 to 2021.
Note: Number of reported cases in southern and northern included cases from bovine, sheep, goats, and other hosts in this period.

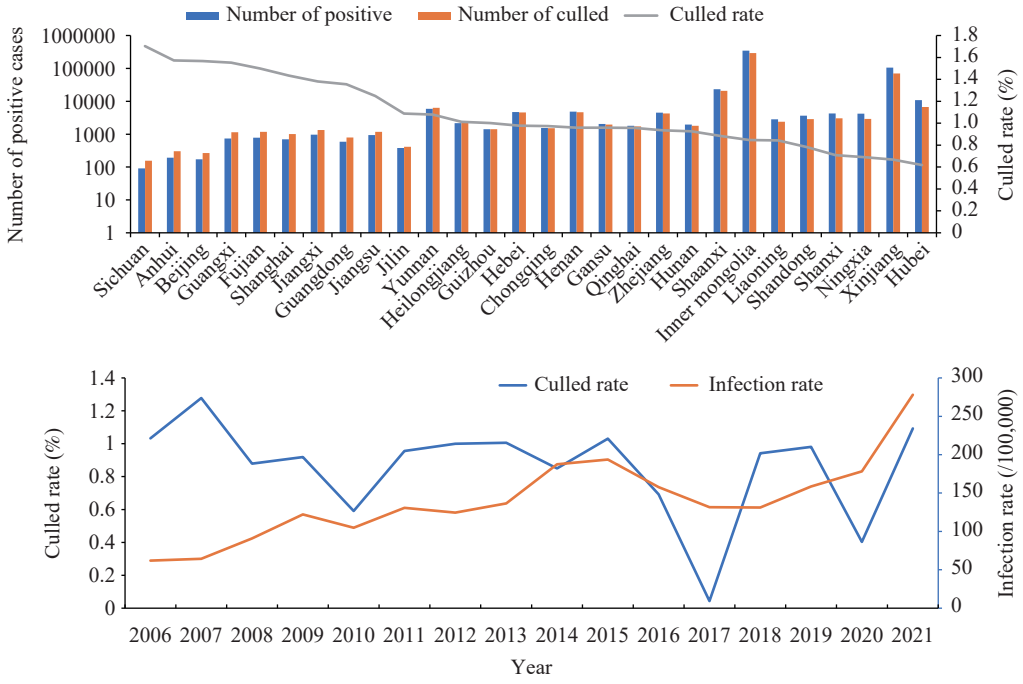

FIGURE 5. Brucellosis in animals from 2006 to 2021. (A) Change trend of culling rates; (B) Infection rates.
Note: Total number of culls in seropositive animals included bovine, sheep, goats, and other hosts each year.

DISCUSSION

This study involved a retrospective epidemiological evolution analysis of brucellosis in animals from the 1950s to the 2020s; the epidemic pattern was similar to that of human brucellosis (*10*). Two epidemic stages were identified during the examined period: the first from the 1950s to the 1980s and the second from 2006 to 2021. Almost all PLADs were involved in both stages, resulting in substantial harm to human health, the farming industry, and socioeconomic development (*9*). This study showed that brucellosis in

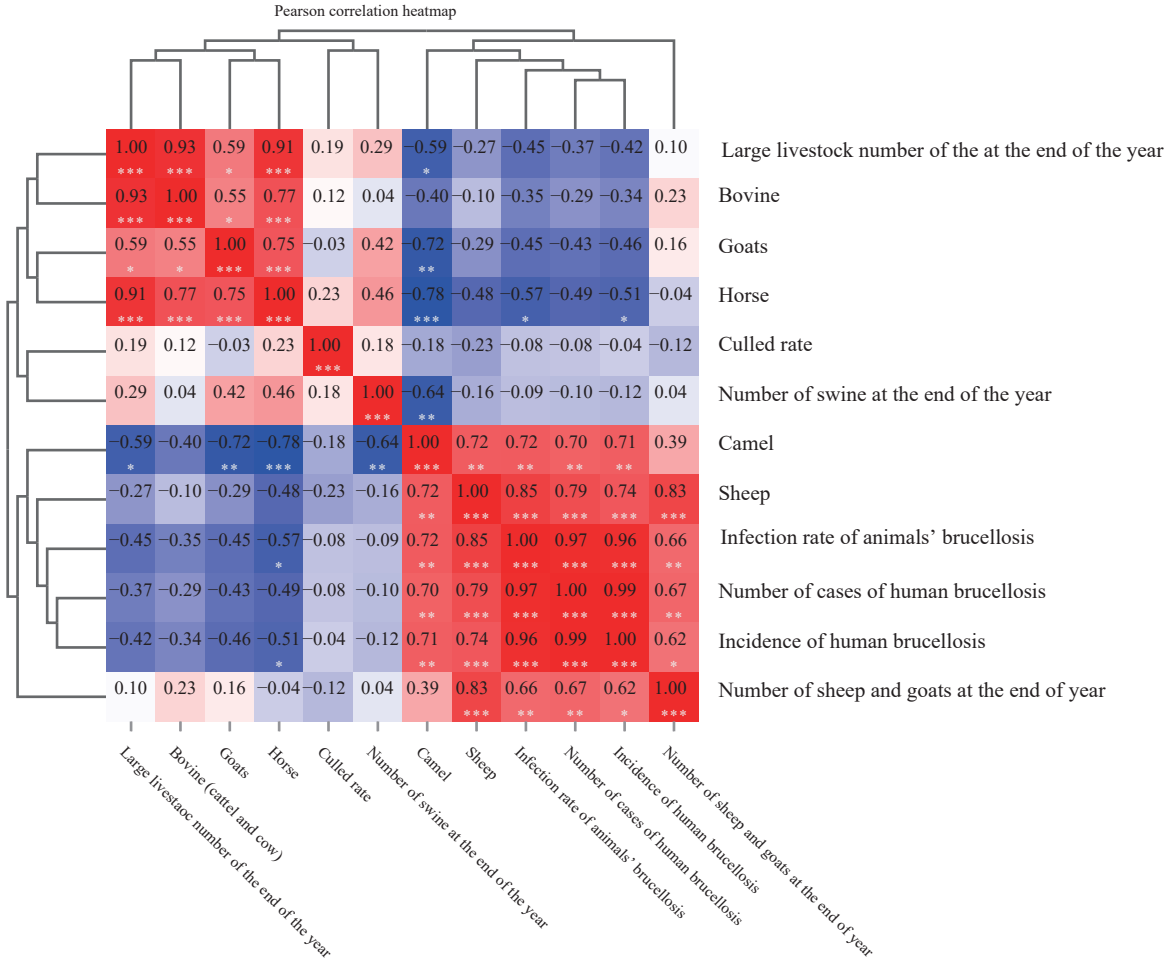

FIGURE 6. Pearson correlation analysis of incidence of human brucellosis and livestock breeding situation.
** $P \leq 0.01$;
*** $P \leq 0.001$.

sheep, goats, and cattle is dominant in mainland China, endemic areas are widespread in most PLADs, and swine brucellosis is predominant in Guangdong and Guangxi. Sheep, goats, and bovines were the only means of production and livelihood for thousands of people from the 1950s to the 1990s; cattle were the main production factor, including for farmland, cultivation, and transportation. After 2000, along with economic development, production pattern changes, and elevated living standards, sheep and goat breeding has continuously increased and expanded, and the incidence of brucellosis has worsened. Swine brucellosis was potentially introduced to mainland China and was dominant in Guangdong and Guangxi, where the breeding industry is large. Surveys showed that swine brucellosis became epidemic on farms and gradually spread to rural areas, further increasing the difficulty of control. In Guangxi, the seropositivity by SAT from 22,127 serum samples from breeding pigs between 2009 and 2011 was under 2.0%, but some historical epidemic areas have a re-emerging risk due to multiple factors (*14*). Currently, the epidemic features of brucellosis display a pronounced change in Guangxi; previously dominant circulating *B. suis* and *B. canis* strains have been replaced by *B. melitensis* strains (*15*).

Since the 1950s, some PLADs with high seroprevalence of animal brucellosis have organized and established institutes and groups for brucellosis surveillance and control according to government planning to implement surveillance and control strategies (*16*). From the 1950s to the 1960s, a set of comprehensive prevention and control measures primarily based on serological testing and vaccine immunization was implemented, including the culling and isolation of positive animals (*16*). In the 1970s, animal immunization was the main control tool, and all animals were vaccinated with the M5 (*17*) or *B. suis* strain 2 (S2) vaccine (*18*). In the 1980s, epidemic

surveillance improved at the national and provincial levels, with the exception of vaccinated animals. Animal brucellosis has been preliminarily controlled since 1986 based on comprehensive control strategies, including immunization, quarantine, elimination, and culling, implemented over the past four decades (*9*,*19*). The incidence of human brucellosis has significantly decreased, and only a few cases have been reported. These data demonstrate that persistent immunization and quarantine measures for animals nationwide are still a priority for stopping human brucellosis (*20*). However, because current detection technology cannot discriminate between infection and vaccine immunization in animals, surveillance in animal immune zones present some puzzles. Therefore, we suggest that the implementation of mass vaccination in small ruminants in high-epidemic areas, and the surveillance and elimination of positive animals, is an option for control measures in zones with a low epidemic (*21*). In Kyrgyzstan, the introduction of mass vaccination in small ruminants has contributed to brucellosis control, thereby reducing the number of infections in animals and humans (*22*). Additionally, a vital reason for brucellosis control in the 1980s was that all breeding farms were collectively owned by the state, facilitating the implementation and purification of prevention and control strategies. Currently, the majority of livestock is owned by individuals, and transportation and transactions are extremely frequent, posing a severe challenge to brucellosis prevention and control (*23*). However, there was a considerable discrepancy in the reported cases between animals and humans, even though there was an almost reversed epidemic trend from 2006 to 2021. The incidence rate of human brucellosis increased during this period; however, the number of reported cases in the animal population gradually declined. These data revealed that testing and surveillance capacity for animal brucellosis was insufficient, and control measures were severely lacking. Testing and culling are very effective measures for animal disease prevention and control (*24*). There was a low positive animal culling rate in some regions with a high incidence rate, meaning that infected animals were not completely eliminated, resulting in the persistent circulation of the disease. The increased infection rate in the south was driven by the introduction of infected animals from the north, implying that control of the infected animal trade and transfer was inadequate. Currently, circulating *Brucella* species have obviously changed. Although a few *B. abrotus*, *B. suis*, and *B. canis* strains were occasionally isolated (*25*–*26*), *B. melitensis* strains were the predominant species in China and have expanded southward (*27*). *B. ovis* has only been historically isolated from Xinjiang; its epidemic situation needs further evaluation (*28*).

Despite incomplete surveillance data hindering accurate and timely prediction of brucellosis trends in animals, the nationwide growth of the animal breeding industry has increased the demand for animal products. Furthermore, the pursuit of economic benefits has driven changes in sheep breeding practices, which is another important factor to consider. For example, the "Small Tailed Han Sheep" breed gained recognition in China for its early maturity, high birth rates, and multiple offspring. This popularity increased the likelihood and frequency of human contact with infected sheep, contributing to the spread and rise in brucellosis infections.

In the Black Sea basin, ruminant health has been hindered by informal animal trade due to economic factors, insufficient support for developing formal trade, and sociocultural drivers (*29*). Animal trade movements were identified as a major transmission route for brucellosis spread between farms (*30*). Therefore, restricting the movement and trade of infected animals and implementing mass vaccination of small ruminants in regions with high incidence have been urged. Furthermore, strengthening surveillance, information exchange, risk assessment, and coordinated response capacity for animal brucellosis is urgent (*31*). In particular, grassroots veterinary departments must screen for and eliminate infected animals in a timely manner. Comprehensive intervention measures against brucellosis incidence in humans and animals are recommended. These measures include public awareness, effective hygiene management, and adequate quarantine or serological detection (e.g., SAT) for newly introduced animals (*32*–*33*). Given the high baseline prevalence, these measures should be based on vaccination combined with measures to promote hygiene and husbandry practices that minimize the risk of brucellosis spreading to low-endemic regions.

CONCLUSION

This study provides an updated epidemiological overview of animal brucellosis nationwide, which will aid government sectors in strengthening routine surveillance and vaccination to reduce disease occurrence and public health risks in China.

Additionally, a vast discrepancy was observed in the incidences of animal and human brucellosis after the 2000s. Therefore, strengthening the surveillance and control of diseased in animals is the most effective strategy. This includes persistent vaccination in high-incidence areas, implementing routine surveillance plans, and using strict animal movement restrictions to restrain further spread.

Conflicts of interest: No conflicts of interest.

Acknowledgments: All authors who have previously published research data on animal brucellosis nationwide and are working on animal brucellosis control and prevention.

Funding: Supported by the National Natural Science Foundation of China (L2124006, Institute internal number: 90100).

doi: 10.46234/ccdcw2024.235

[#] Corresponding author: Zhenjun Li, lizhenjun@icdc.cn.

[1] National Key Laboratory of Intelligent Tracking and Forecasting for Infectious Diseases, National Institute for Communicable Disease Control and Prevention, Chinese Center for Disease Control and Prevention, Beijing, China; [2] Ulanqab Center for Disease Control and Prevention, Jining City, Inner Mongolia Autonomous Region, China; [3] Tongliao Center for Disease Control and Prevention, Horqin City, Inner Mongolia Autonomous Region, China; [4] Chinese Center for Disease Control and Prevention, Beijing, China.

Submitted: January 24, 2024; Accepted: September 02, 2024

REFERENCES

1. Donev DM. Brucellosis as priority public health challenge in south eastern European countries. Croat Med J 2010;51(4):283 – 4. https://doi.org/10.3325/cmj.2010.51.283.
2. Pisarenko SV, Kovalev DA, Volynkina AS, Ponomarenko DG, Rusanova DV, Zharinova NV, et al. Global evolution and phylogeography of *Brucella melitensis* strains. BMC Genomics 2018;19(1):353. https://doi.org/10.1186/s12864-018-4762-2.
3. Rossetti CA, Maurizio E, Rossi UA. Comparative review of brucellosis in small domestic ruminants. Front Vet Sci 2022;9:887671. https://doi.org/10.3389/fvets.2022.887671.
4. Liu ZG, Wang CL, Wei KJ, Zhao ZZ, Wang M, Li D, et al. Investigation of genetic relatedness of *Brucella* strains in countries along the silk road. Front Vet Sci 2021;7:539444. https://doi.org/10.3389/fvets.2020.539444.
5. Liu ZG, Gao LP, Wang M, Yuan M, Li ZJ. Long ignored but making a comeback: a worldwide epidemiological evolution of human brucellosis. Emerg Microbes Infect 2024;13(1):2290839. https://doi.org/10.1080/22221751.2023.2290839.
6. Mazlina M, Khairani-Bejo S, Hazilawati H, Tiagarahan T, Shaqinah NN, Zamri-Saad M. Pathological changes and bacteriological assessments in the urinary tract of pregnant goats experimentally infected with *Brucella melitensis*. BMC Vet Res 2018;14(1):203. https://doi.org/10.1186/s12917-018-1533-x.
7. Bagheri Nejad R, Krecek RC, Khalaf OH, Hailat N, Arenas-Gamboa AM. Brucellosis in the Middle East: current situation and a pathway forward. PLoS Negl Trop Dis 2020;14(5):e0008071. https://doi.org/10.1371/journal.pntd.0008071.
8. Garofolo G, Fasanella A, Di Giannatale E, Platone I, Sacchini L, Persiani T, et al. Cases of human brucellosis in Sweden linked to Middle East and Africa. BMC Res Notes 2016;9:277. https://doi.org/10.1186/s13104-016-2074-7.
9. Shang DQ, Xiao DL, Yin JM. Epidemiology and control of brucellosis in China. Vet Microbiol 2002;90(1-4):165 – 82. https://doi.org/10.1016/s0378-1135(02)00252-3.
10. Lai SJ, Zhou H, Xiong WY, et al. Changing epidemiology of human brucellosis, China, 1955-2014. Emerg Infect Dis 2017;23(2):184 – 94. https://doi.org/10.3201/eid2302.151710.
11. Yang HM, Chen QL, Li Y, Mu D, Zhang YP, Yin WW. Epidemic characteristics, high-risk areas and space-time clusters of human brucellosis - China, 2020-2021. China CDC Wkly 2023;5(1):17 – 22. https://doi.org/10.46234/ccdcw2023.004.
12. Mu HY, Chen JZ, Huang WJ, Huang G, Deng MY, Hong SM, et al. OmicShare tools: a zero‐code interactive online platform for biological data analysis and visualization. iMeta 2024;3(5):e228. https://doi.org/10.1002/IMT2.228.
13. Tao ZF, Yang ZP, Chen YS, Yang SF, Xu JC, Wang Y, et al. Epidemiological survey of first human brucellosis outbreak caused by the Sika deer (*Cervus nippon*) - Guizhou Province, China, 2019. China CDC Wkly 2021;3(14):301 – 3. https://doi.org/10.46234/ccdcw2021.081.
14. Huang ZX, Chen YH, Lu JH, Liang YY, Zuo WS, Zhou GJ, et al. Epidemiological investigation and analysis of brucellosis in Guangxi pig breeds. Chin J Epidemiol 1986;5(1):48-51. https://kns.cnki.net/KCMS/detail/detail.aspx?dbcode=CJFQ&filename=ZDFB198601017. (In Chinese).
15. Liu ZG, Wang M, Zhao HY, Piao DR, Jiang H, Li ZJ. Investigation of the molecular characteristics of *Brucella* isolates from Guangxi Province, China. BMC Microbiol 2019;19(1):292. https://doi.org/10.1186/s12866-019-1665-6.
16. Shang DQ. Progress in the study of prevention and control of Brucellosis in China in last 50 years. Chin J Epidemiol 2000;21(1):55 – 7. https://doi.org/10.3760/j.issn:0254-6450.2000.01.018.
17. Hou HH, Liu XF, Peng QS. The advances in brucellosis vaccines. Vaccine 2019;37(30):3981 – 8. https://doi.org/10.1016/j.vaccine.2019.05.084.
18. Zhu LQ, Feng Y, Zhang G, Jiang H, Zhang Z, Wang N, et al. *Brucella suis* strain 2 vaccine is safe and protective against heterologous *Brucella* spp. infections. Vaccine 2016;34(3):395 – 400. https://doi.org/10.1016/j.vaccine.2015.09.116.
19. Yang HX, Zhang SW, Wang TJ, Zhao CH, Zhang XY, Hu J, et al. Epidemiological characteristics and spatiotemporal trend analysis of human brucellosis in China, 1950-2018. Int J Environ Res Public Health 2020;17(7):2382. https://doi.org/10.3390/ijerph17072382.
20. Almuzaini AM. An epidemiological study of brucellosis in different animal species from the Al-Qassim Region, Saudi Arabia. Vaccines (Basel) 2023;11(3):694. https://doi.org/10.3390/vaccines11030694.
21. Herrera-López E, Suárez-Güemes F, Hernández-Andrade L, Córdova-López D, Díaz-Aparicio E. Epidemiological study of Brucellosis in cattle, immunized with *Brucella abortus* RB51 vaccine in endemic zones. Vaccine 2010;28 Suppl 5:F59-63. http://dx.doi.org/10.1016/j.vaccine.2010.03.057.
22. Kydyshov K, Usenbaev N, Sharshenbekov A, Aitkuluev N, Abdyraev M, Chegirov S, et al. Brucellosis in humans and animals in Kyrgyzstan. Microorganisms 2022;10(7):1293. https://doi.org/10.3390/MICROORGANISMS10071293.
23. Zeng H, Wang YM, Sun XD, Liu P, Xu QG, Huang D, et al. Status and influencing factors of farmers' private investment in the prevention and control of sheep brucellosis in China: a cross-sectional study. PLoS Negl Trop Dis 2019;13(3):e0007285. https://doi.org/10.1371/journal.pntd.0007285.
24. Nie YB, Sun XD, Hu HP, Hou Q. Bifurcation analysis of a sheep brucellosis model with testing and saturated culling rate. Math Biosci

Eng 2023;20(1):1519 – 37. https://doi.org/10.3934/mbe.2023069.
25. Wang H, Xu WM, Zhu KJ, Zhu SJ, Zhang HF, Wang J, et al. Molecular investigation of infection sources and transmission chains of brucellosis in Zhejiang, China. Emerg Microbes Infect 2020;9(1):889 – 99. https://doi.org/10.1080/22221751.2020.1754137.
26. Liu ZG, Wang LJ, Piao DR, Wang M, Liu RH, Zhao HY, et al. Molecular investigation of the transmission pattern of *Brucella suis* 3 from Inner Mongolia, China. Front Vet Sci 2018;5:271. https://doi.org/10.3389/fvets.2018.00271.
27. Zhu X, Zhao ZZ, Ma SY, Guo ZW, Wang M, Li ZJ, et al. *Brucella melitensis*, a latent "travel bacterium," continual spread and expansion from northern to Southern China and its relationship to worldwide lineages. Emerg Microbes Infect 2020;9(1):1618 – 27. https://doi.org/10.1080/22221751.2020.1788995.
28. Wang YZ, Chen CF, Cui BY, Liu JX. Comparative study on identity of *B.ovis* 019 strain by traditional methods and HOOF-prints technique. Acta Microbiol Sin 2007;47(2):240 – 3. https://doi.org/10.3321/j.issn:0001-6209.2007.02.011.
29. Arede M, Beltrán-Alcrudo D, Aliyev J, Chaligava T, Keskin I, Markosyan T, et al. Examination of critical factors influencing ruminant disease dynamics in the Black Sea Basin. Front Vet Sci 2023;10:1174560. https://doi.org/10.3389/fvets.2023.1174560.
30. Darbon A, Valdano E, Poletto C, Giovannini A, Savini L, Candeloro L, et al. Network-based assessment of the vulnerability of Italian regions to bovine brucellosis. Prev Vet Med 2018;158:25 – 34. https://doi.org/10.1016/j.prevetmed.2018.07.004.
31. Batsukh Z, Tsolmon B, Otgonbaatar D, Undraa B, Dolgorkhand A, Ariuntuya O. One health in Mongolia. In: Mackenzie JS, Jeggo M, Daszak P, Richt JA, editors. One health: the human-animal-environment interfaces in emerging infectious diseases. Berlin, Heidelberg: Springer. 2012; p. 123-37. http://dx.doi.org/10.1007/82_2012_253.
32. Merga Sima D, Abdeta Ifa D, Merga AL, Tola EH. Seroprevalence of bovine brucellosis and associated risk factors in western Ethiopia. Vet Med (Auckl) 2021;12:317 – 24. https://doi.org/10.2147/VMRR.S338930.
33. Moriyón I, Blasco JM, Letesson JJ, De Massis F, Moreno E. Brucellosis and one health: inherited and future challenges. Microorganisms 2023;11(8):2070. https://doi.org/10.3390/MICROORGANISMS11082070.

SUPPLEMENTARY MATERIAL

SUPPLEMENTARY TABLE S1. Distribution pattern of *Brucella* strains in 23 provinces from 1978 to 2019.

PLADs	Distribution pattern of *Brucella* strains from 1978 to 1989						Distribution pattern of *Brucella* strains from 1996 to 2019			
	B. melitensis	*B. abortus*	*B. suis*	*B. canis*	*B. ovis*	Total	*B. melitensis*	*B. abortus*	*B. suis*	Total
Hunan	–	1	1	1	–	3	–	–	–	–
Yunnan	4	2	1	–	–	7	–	–	–	–
Fujian	5	1	2	6	–	14	–	–	–	–
Heilongjiang	36	1	1	–	–	38	–	10	–	10
Shandong	53	–	–	–	–	53	12	–	–	0
Inner Mongolia	62	10	1	–	–	73	78	–	22	100
Guangdong	–		90	3	–	93	–	–	–	0
Qinghai	97	–	–	–	–	97	14	–	1	15
Ningxia	95	–	7	–	–	102	–	–	–	0
Xizang	87	14	2	–	–	103	–	–	–	0
Henan	109	1	–	–	–	110	2	–	–	2
Guangxi	7	–	98	6	–	111	–	–	–	0
Shanxi	119	1	1	–	–	121	1	–	–	1
Gansu	114	8	2	–	–	124	26	–	–	26
Sichuan	25	122	–	9	–	156	–	–	–	0
Shaanxi	207	3	–	–	–	210	–	–	–	0
Jilin	217	30	–	–	–	247	–	–	–	0
Xinjiang	286	56	2	7	2	353	101	5	–	106
Chongqing	–	–	–	–	–	–	3	–	–	3
Guizhou	–	–	–	–	–	–	3	–	–	3
Hainan	–	–	–	–	–	–	1	–	–	1
Hebei	–	–	–	–	–	–	5	11	–	16
Zhejiang	–	–	–	–	–	–	8		–	8

Note: "–" means no strain.
Abbreviation: PLADs=provincial-level administrative divisions.

Youth Editorial Board

Indexed by Science Citation Index Expanded (SCIE), Social Sciences Citation Index (SSCI), PubMed Central (PMC), Scopus, Chinese Scientific and Technical Papers and Citations, and Chinese Science Citation Database (CSCD)

The inauguration of *China CDC Weekly* is in part supported by Project for Enhancing International Impact of China STM Journals Category D (PIIJ2-D-04-(2018)) of China Association for Science and Technology (CAST).

CCDC weekly

Vol. 6 No. 44 Nov. 1, 2024

Responsible Authority
National Disease Control and Prevention Administration

Sponsor
Chinese Center for Disease Control and Prevention

Editing and Publishing
China CDC Weekly Editorial Office
No.155 Changbai Road, Changping District, Beijing, China
Tel: 86-10-63150501, 63150701
Email: weekly@chinacdc.cn

CSSN
ISSN 2096-7071 (Print)
ISSN 2096-3101 (Online)
CN 10-1629/R1